Operando (micro) XAFS analysis

Iztok Arčon [1,2]

Robert Dominko [3],
Katarina Vogel-Mikuš [4,2]

[1] University of Nova Gorica, Vipavska 13, POB 301, Nova Gorica, Slovenia
[2] J. Stefan Institute, Jamova 39, P. P. 3000, Ljubljana, Slovenia
[3] National institute of Chemistry, P.O.B. 660, SI-1001 Ljubljana, Slovenia
[4] Biotechnical Faculty, University of Ljubljana, Ljubljana, Slovenia

X-ray absorpcon spectroscopy

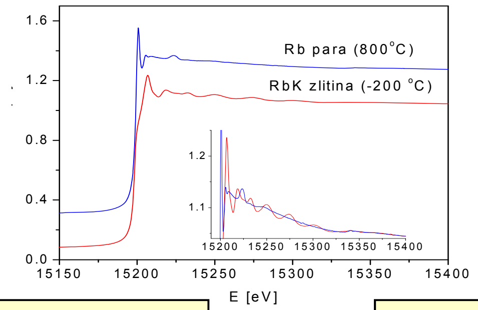

Basic research

Applied research

Exsperimental analysis of colectiv dynamics in atoms

Structural analysis of materials

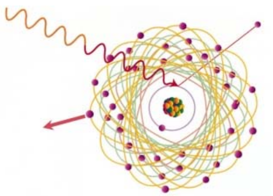

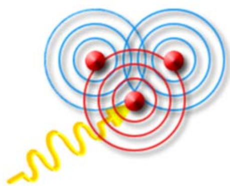

- Multielectron photoexcitations.
- Study of correlations and collecive proceses in multielectron atomic systems.
- Measuring absolute cross sections for photoeffect in inner shells.

Determination of atomic and molecular structure od materials.

Li-oin batteries, cataliysts, nanomaterials, ferroelectric ceramics, biological and environmental samples, …

X-ray Absorption spectroscopy

Measurements of energy dependence of the absorption coefficient μ(E)

TRANSMITION DETECTION MODE:

$$I = I_0 \, e^{-\mu d}$$

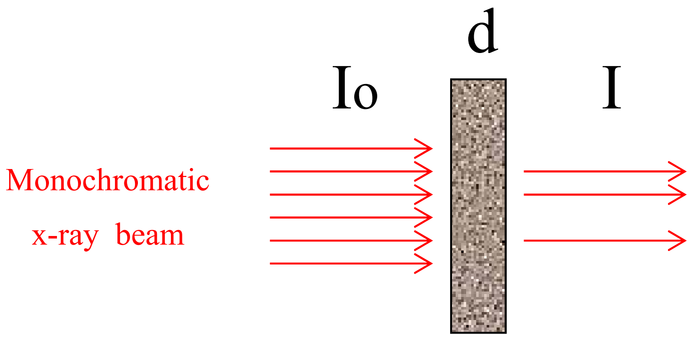

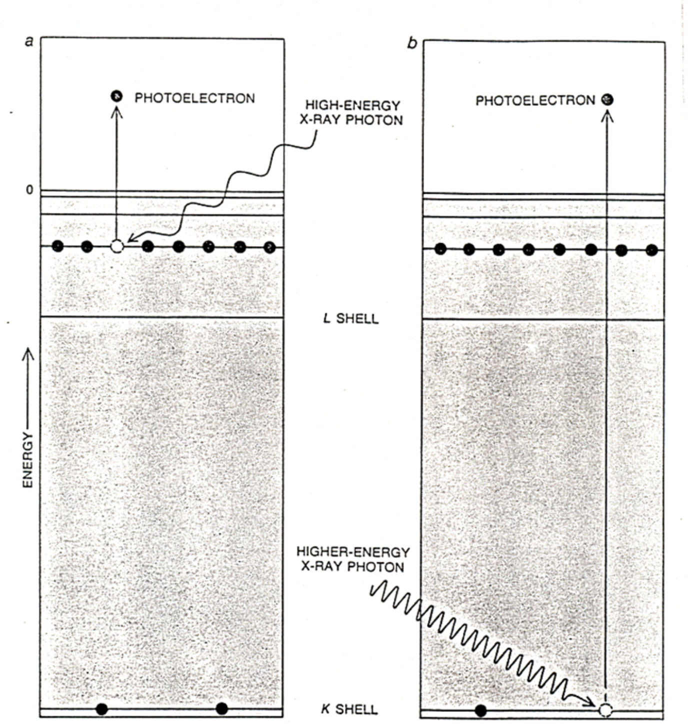

Optimal absorption thickness $\mu d \approx 2$

Typical sample thickness for metal foils (Cr, Fe, Co, Ni, Cu, Zn) is ~ 5 μm

Total Electron Yield Or Fluorescence Detection Mode

Use: - thin films on thick substrate
- diluted samples,

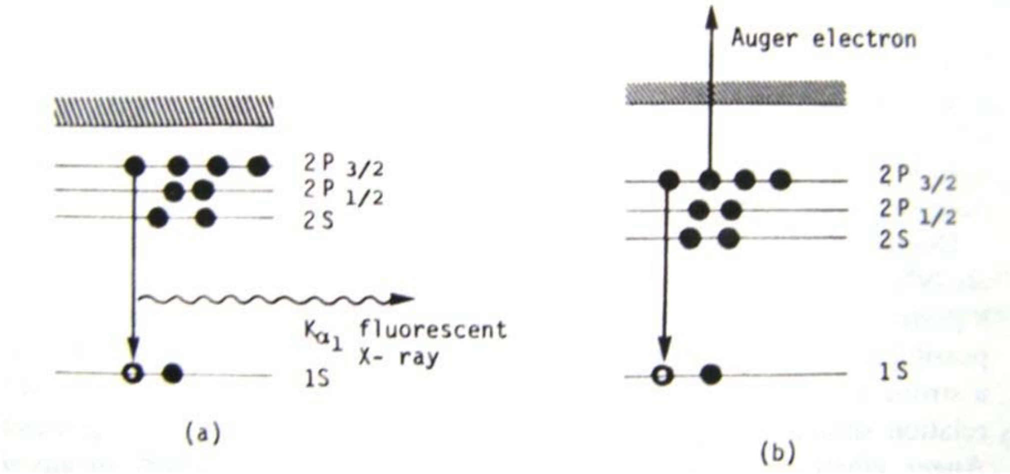

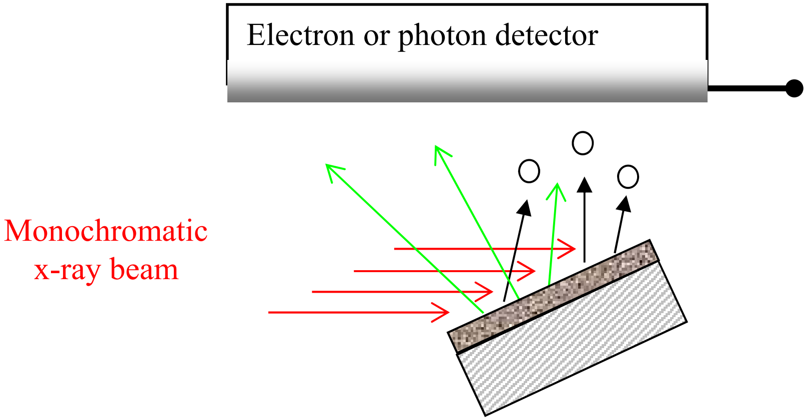

$$I \propto I_0 \varepsilon \omega \Omega x \mu$$

μ –absorption coefficient
x –layer thickness
ω –radiative or nonradiative yield
Ω –solid angle of collection
ε – detection efficiency

Investigated depth:

Electrons: ~ 100 nm
Photons: d ≈ 1/ μ μm to mm range

The I_o signal has to be corrected for a specific gas and preasure of the first ionisation cell. The correction factor can be calculated by ATOMS program.

X-ray absorption spectrum **μ(E)** in the energy range of K and L absorption edges provides information on local structure around investigated atoms

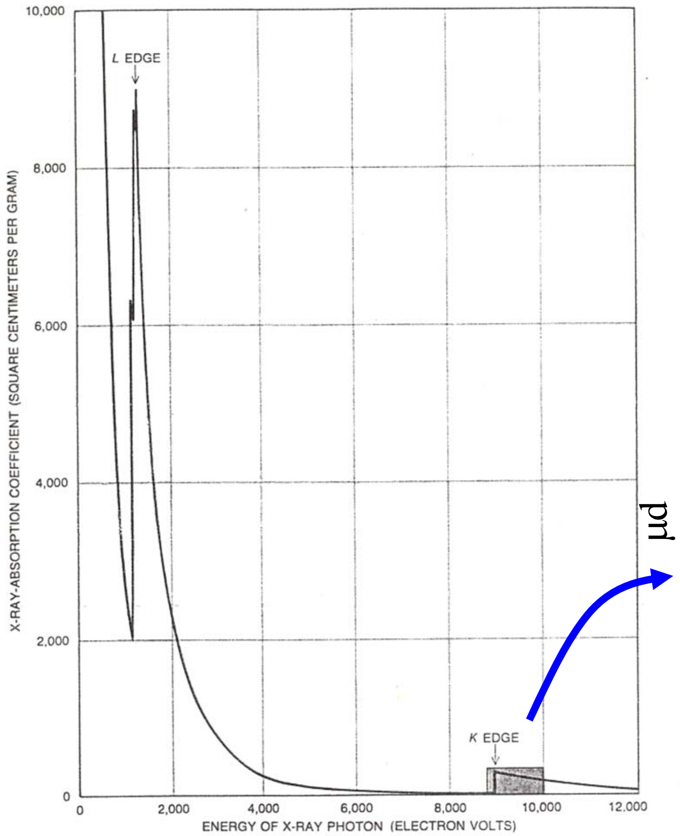

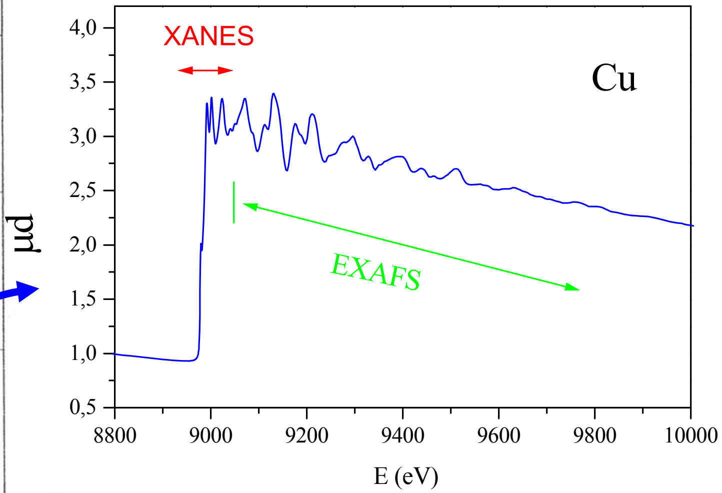

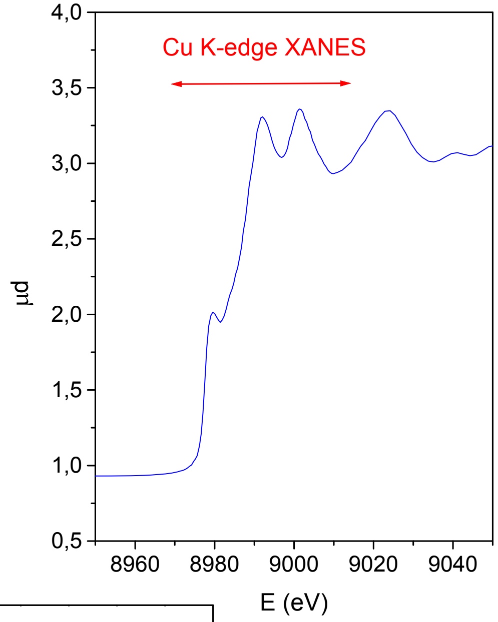

EXAFS: "Microscope" to observe local neighboorhood of selected elements in any material

Rhodium (Rh)
metal foil,
fcc crystal structure

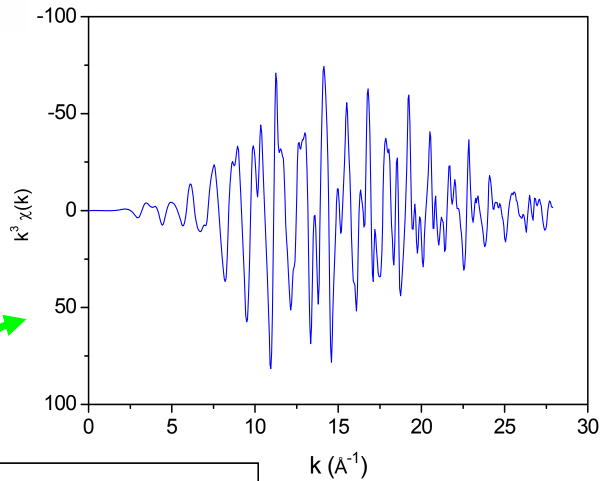

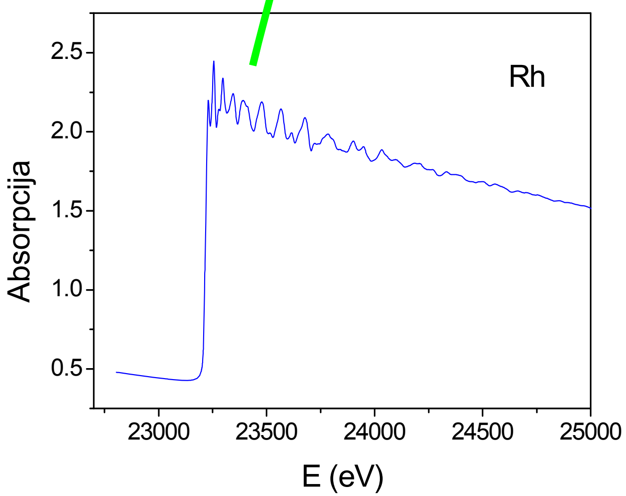

Fourier transform

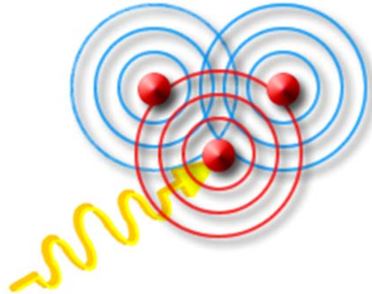

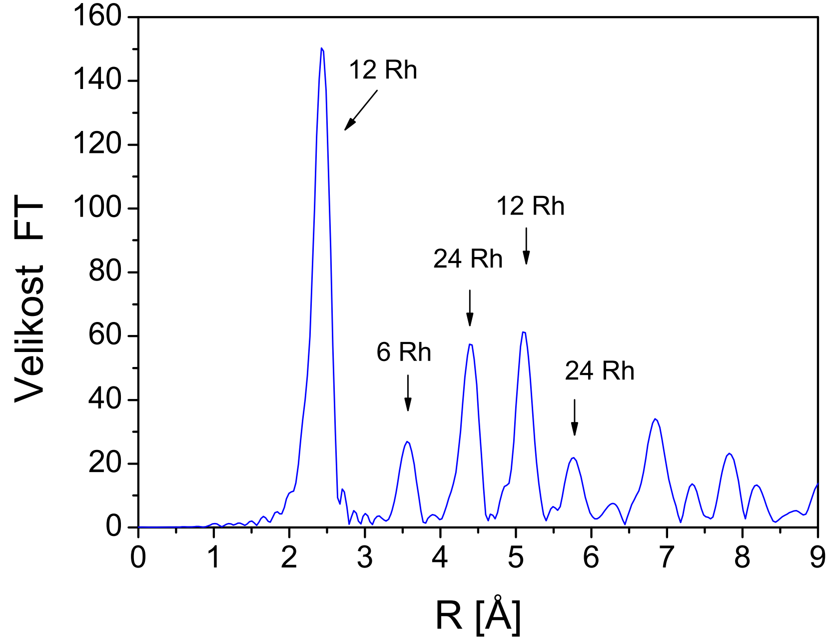

XANES

Contains information about unoccupied valence orbitals of the absorbing atom.

It can be used to identify simmetry and valence state of the absorbing atom.

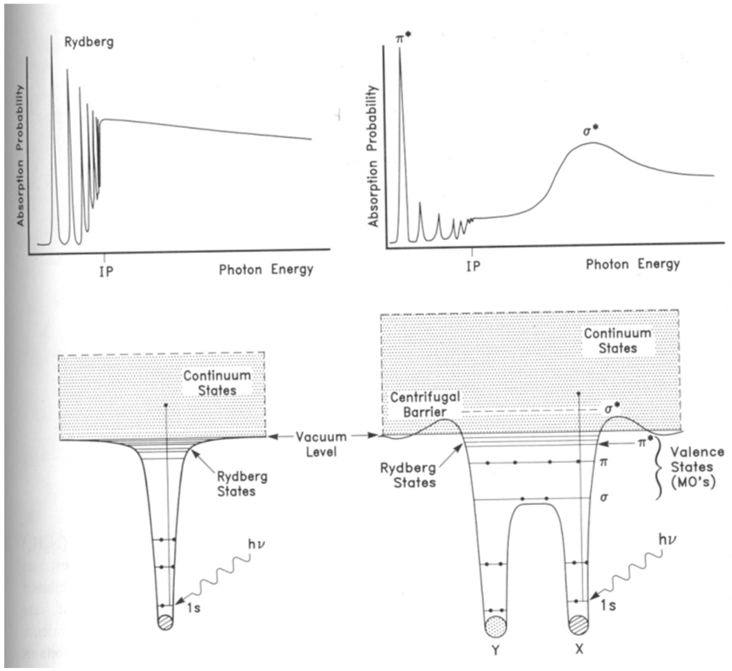

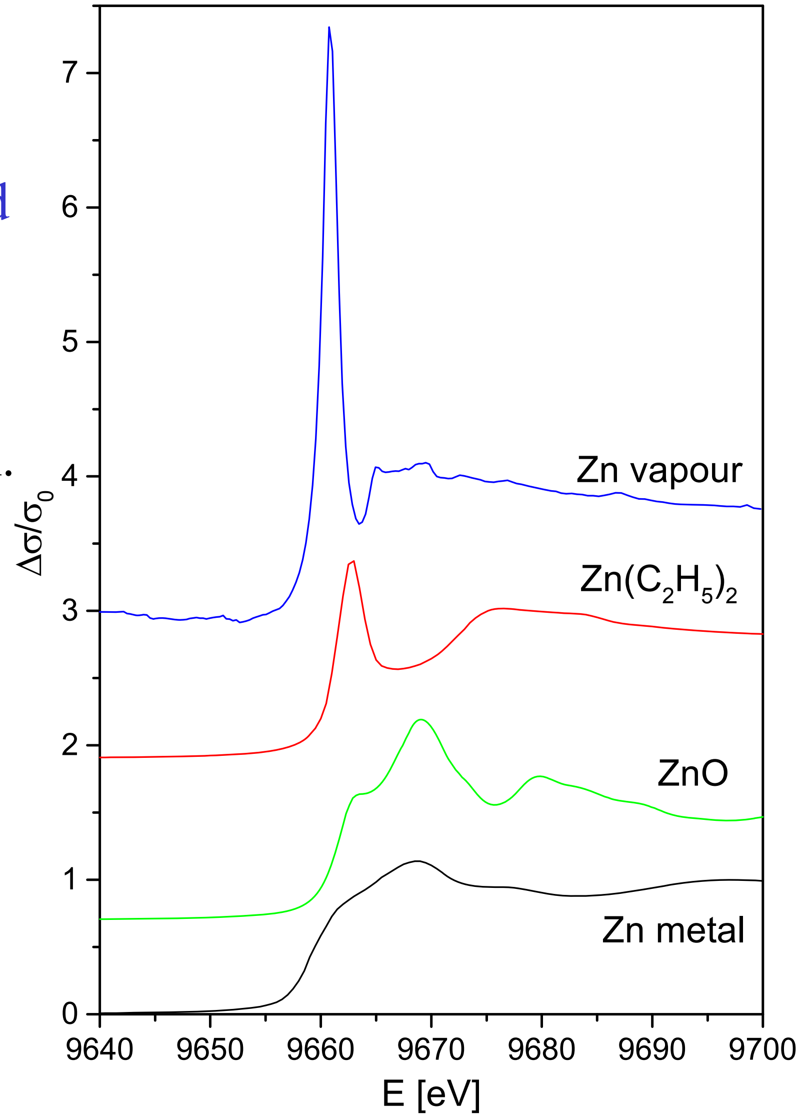

Zn K-edge XANES spectra measured on free and bound Zn atoms.

Operando XAS analysis on Li-ion batteries
Motivation

- Searching for new cathode materials for high energy Li-ion batteries with fully reversible lithium extraction that can deliver high battery capacitiy.
- Operando XANES and EXAFS analysis as **a tool to monitor gradual changes of oxidation state and local structure** of transition-metal cations during lithium exchange, i.e. during charging and discharging of the Li-ion battery.
- Provide the information on the dynamics of the battery operation on the atomic level and clarify the role of transition-metal cations (Fe, Mn, V) in the electrochemical activity of the material. Determine the degree of reversibility of the process in one or several cycles.

Aim of in-operando XAS

- Operando XANES and EXAFS analysis as **a tool to monitor gradual changes of oxidation state and local structure** of transition-metal cations during lithium exchange, i.e. during charging and discharging of the Li-ion battery.

- Provide the information on the dynamics of the battery operation on the atomic level and clarify the role of transition-metal cations (Fe, Mn, V) in the electrochemical activity of the material. Determine the degree of reversibility of the process in one or several cycles.

$Li_2(Fe_{0.8}Mn_{0.2})SiO_4$ cathode meterial

XRD data :

- Monoclinic crystal structure with *P121/n1* space group. a = 8.245 Å, b = 5.018 Å and c = 8.246 Å
- The structure is composed of MnO_4, FeO_4, SiO_4 and LiO_4 tetrahedra.
- The crystal structure contains empty octahedral interstitial cavities that form empty channels, which enables transport of Li^+ ions.

Advantages:

- High capacity (200 mAh/g at a C/50 cycling rate)
- Good thermal stability

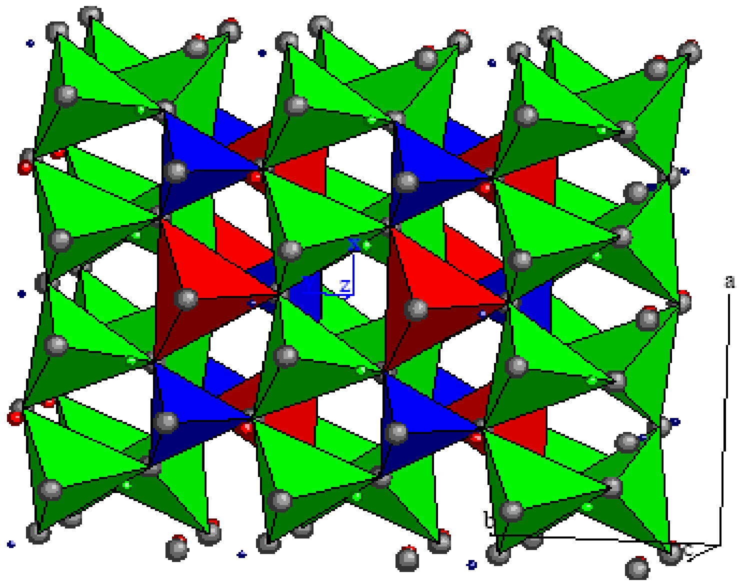

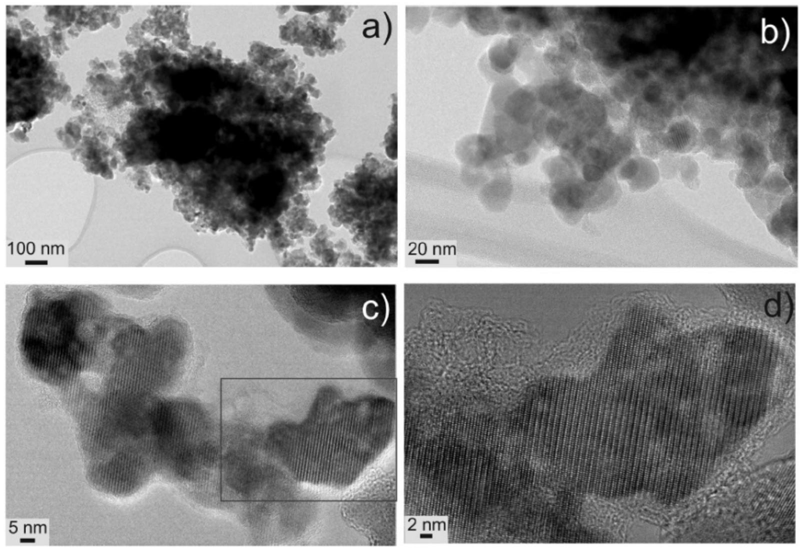

Charge / discharge curves in the first cycle at C/15 current density at 60 oC. Exchanged of 1 mol Li.

R. Dominko, M. Bele, M. Gaberšček, A. Meden, M. Remškar, and J. Jamnik, *Electrochem. Commun.* **8**, 217 (2006).

Operando XAS experiment

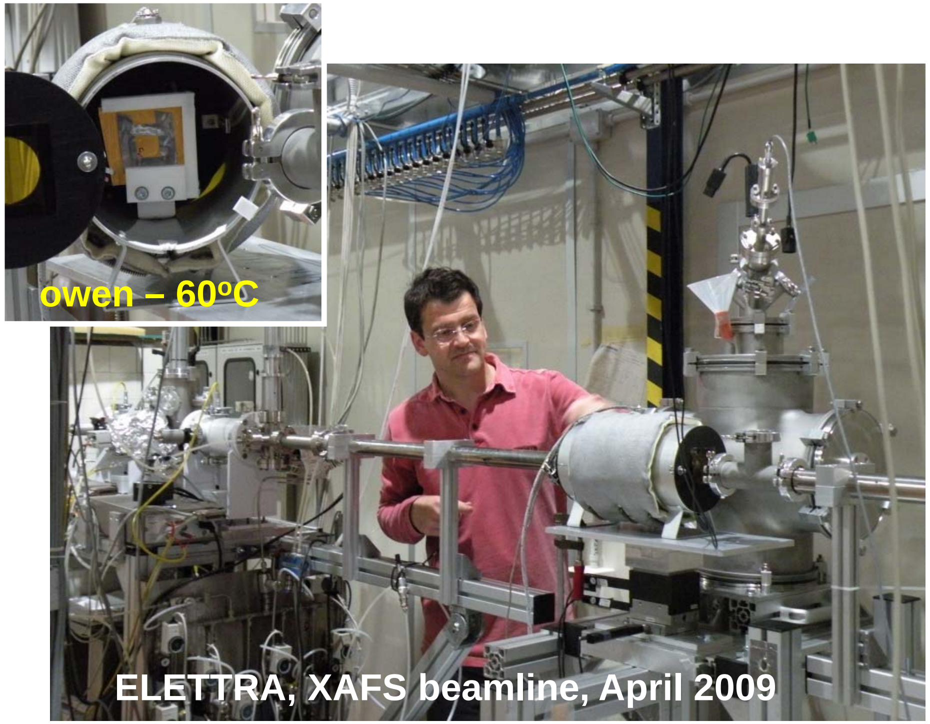

Half-battery sealed in triplex foil:

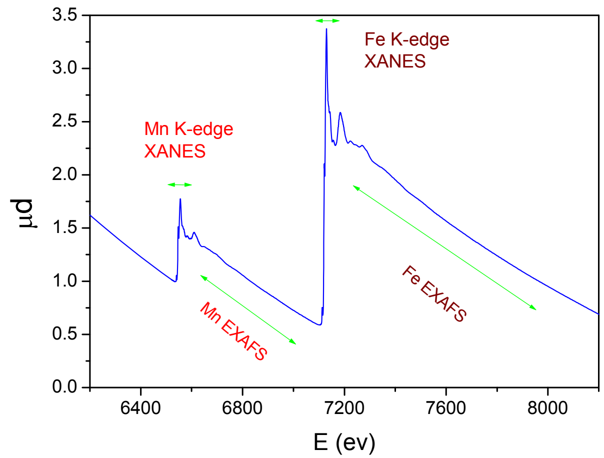

Fe and Mn XANES and EXAFS spectra were measured in time intervals of of 55 min.

- **Li_2FeTiO_4** charging (411min), discharging (192 min) at RT with C/10 current density in time intervals of 25 min.
- **$Li_2Fe_{0.8}Mn_{0.2}SiO_4$: In situ charging (908 min), discharging (852 min) at 60 ºC with C/15 current density** in time intervals of 50 min
- XAFS beamline at ELETTRA and C beamline in HASYLAB at DESY, Hamburg. A Si(111) double crystal monochromator with about 1 eV energy resolution at Fe k-edge (7112 eV) was used. Exact energy calibration with simultaneous absorption measurements on a 5 mm thick V, Fe or Mn metal foil. Absolute energy reproducibility of the measured spectra was ±0.05 eV.

$Li_{2-x}Fe_{0.8}Mn_{0.2}SiO_4$

battery charging

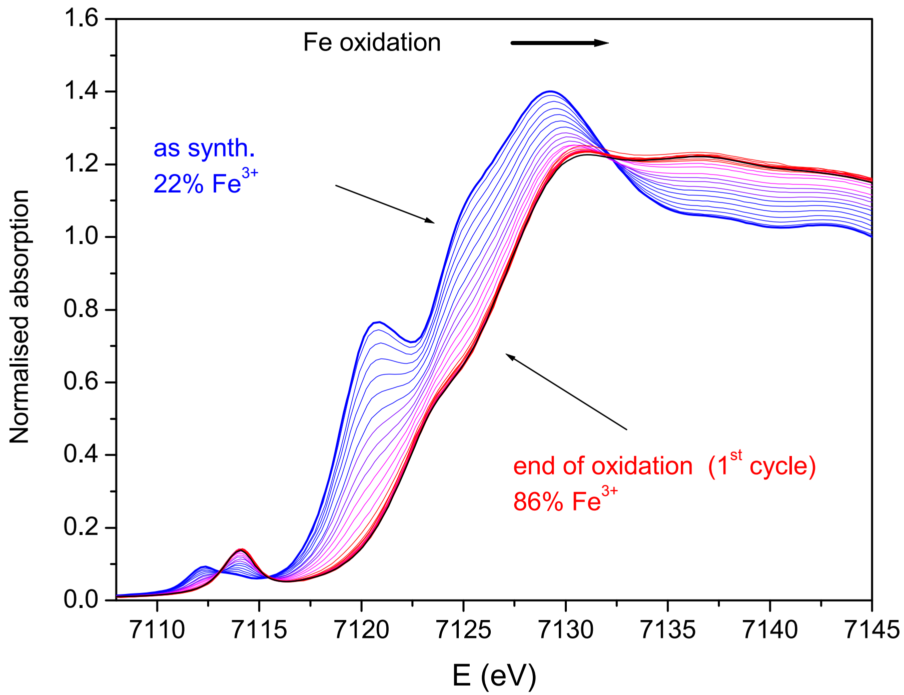

battery discharging

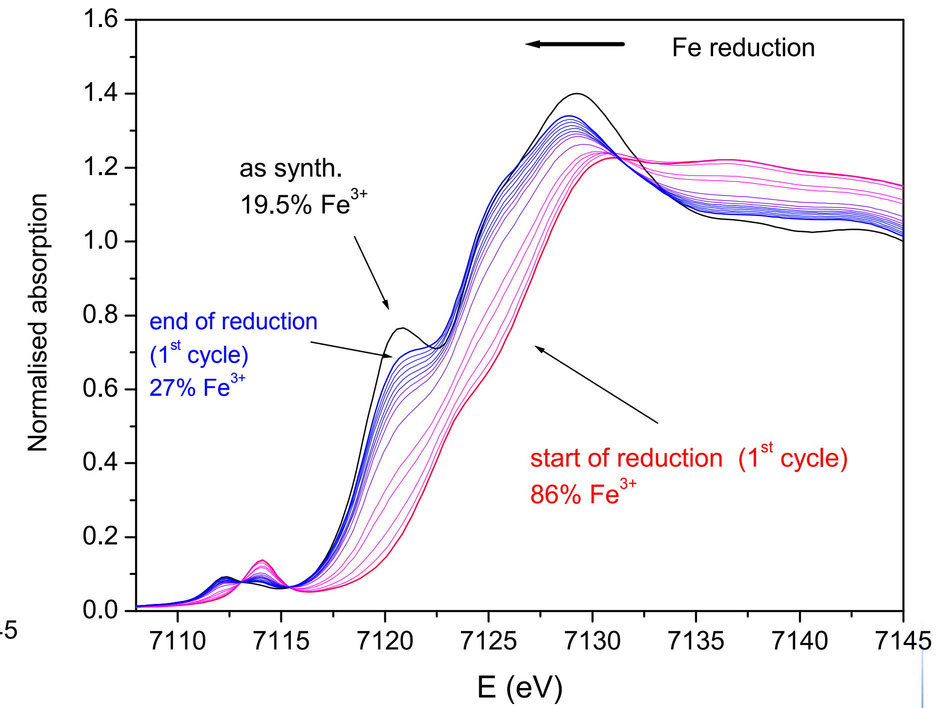

R. Dominko, C. Sirisopanaporn, C. Masquelier, D. Hanzel, I. Arcon, M. Gabersceka, Journal of The Electrochemical Society, 157 12 A1309-A1316 (2010)

$Li_{2-x}Fe_{0.8}Mn_{0.2}SiO_4$

battery charging

Mn oxidation

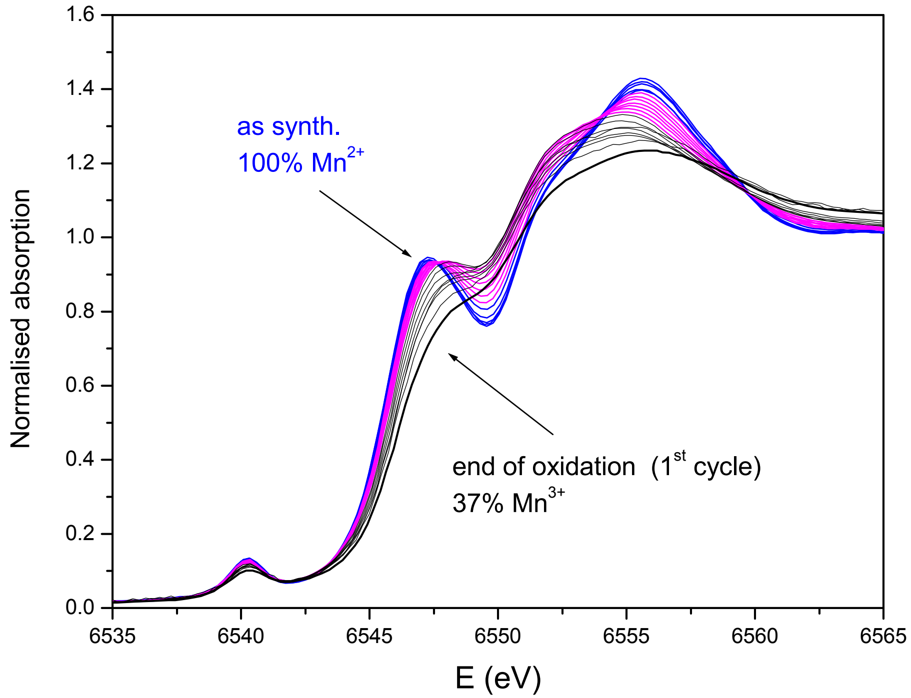

battery discharging

Mn reduction

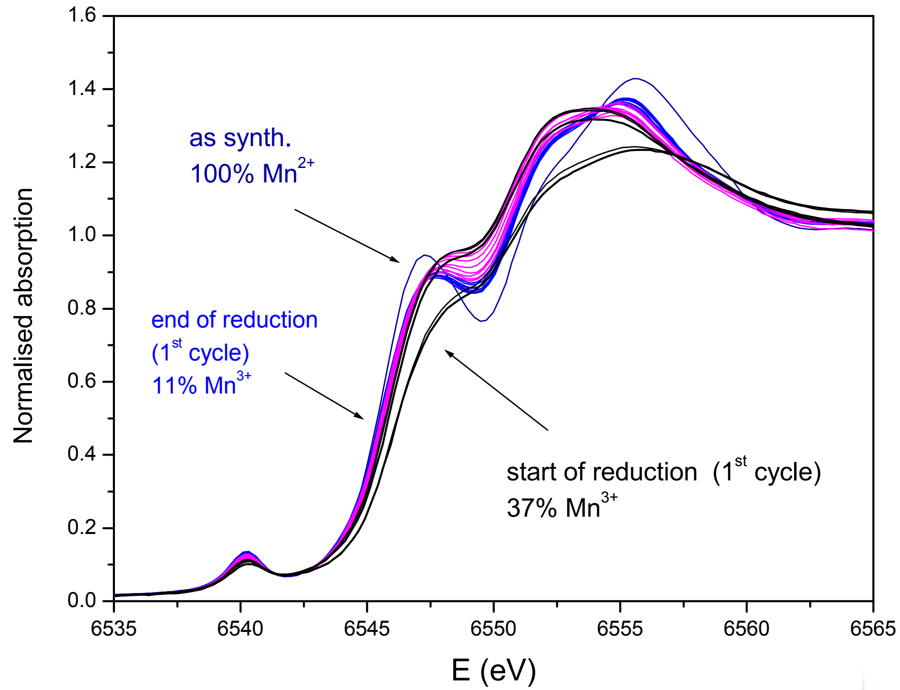

R. Dominko, C. Sirisopanaporn, C. Masquelier, D. Hanzel, I. Arcon, M. Gabersceka, Journal of The Electrochemical Society, 157 12 A1309-A1316 (2010)

$Li_{2-x}Fe_{0.8}Mn_{0.2}SiO_4$

Linear combination fit

of XANES spectra of intermediate states with the spectra of the starting and the most charged state.

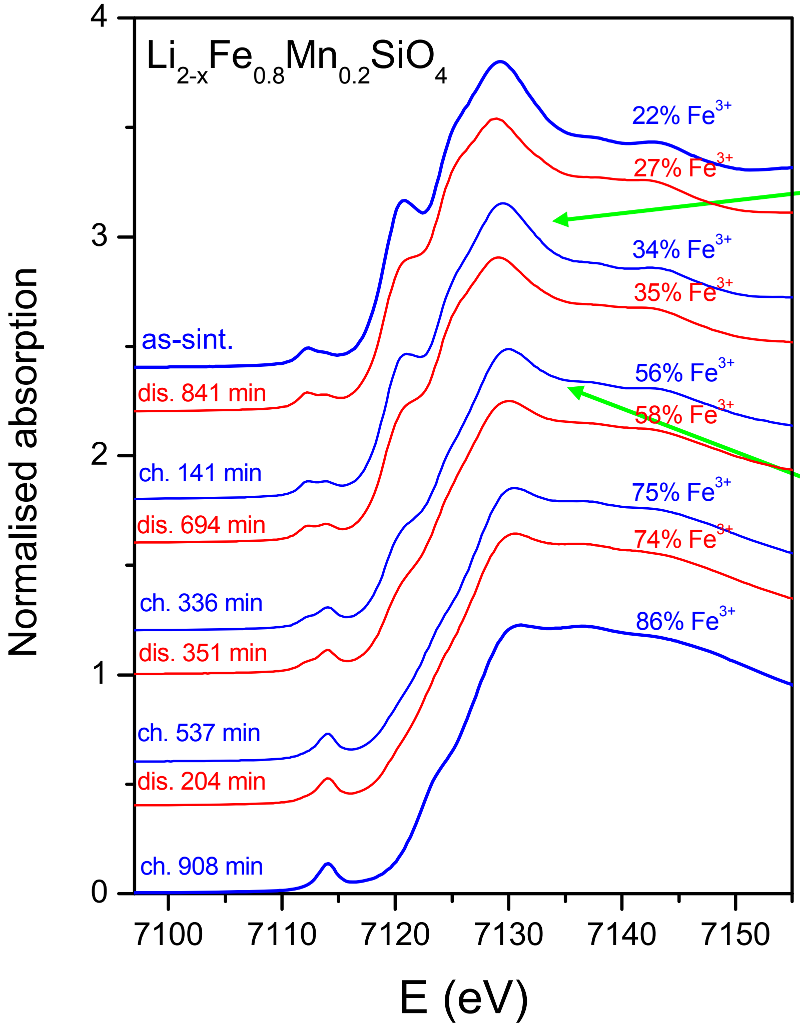

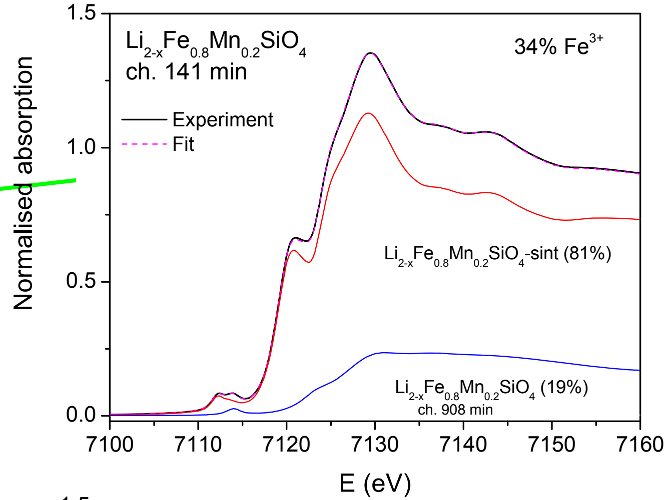

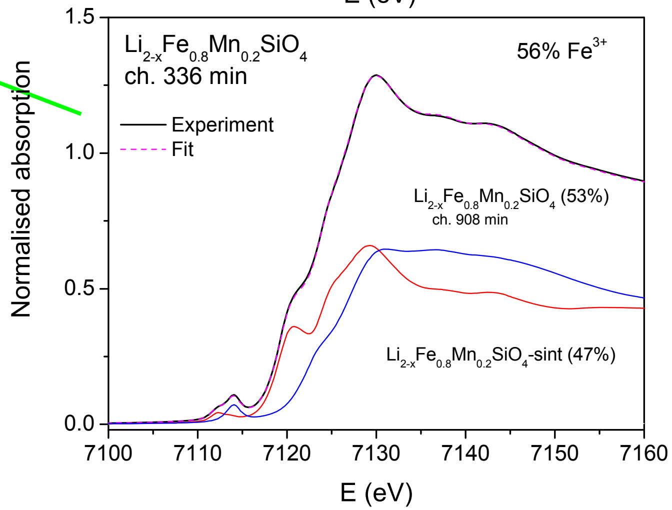

$Li_{2-x}Fe_{0.8}Mn_{0.2}SiO_4$

Linear combination fit with XANES spectra of "as-sint." and "ch. 908 min"

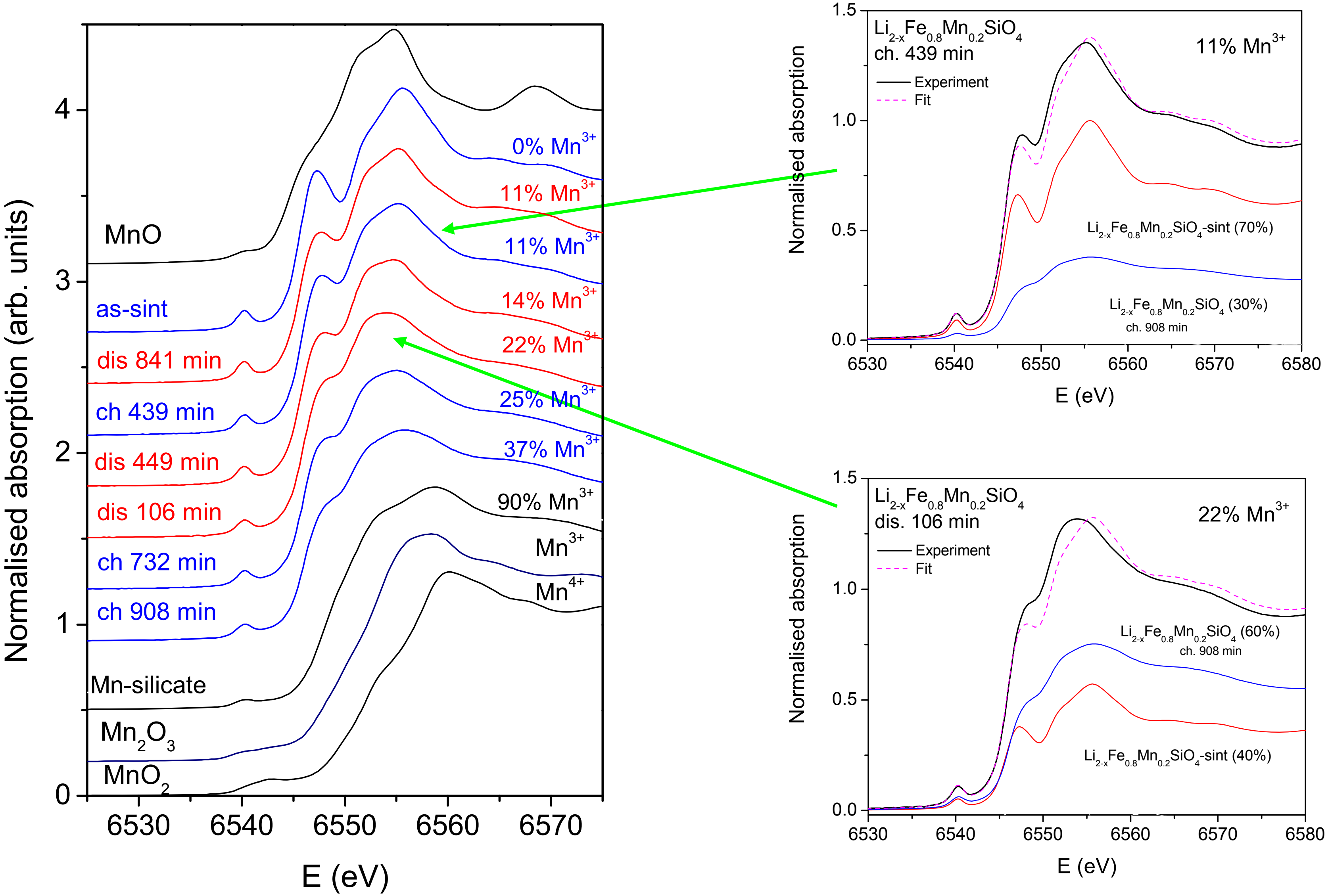

$Li_{2-x}Fe_{0.8}Mn_{0.2}SiO_4$

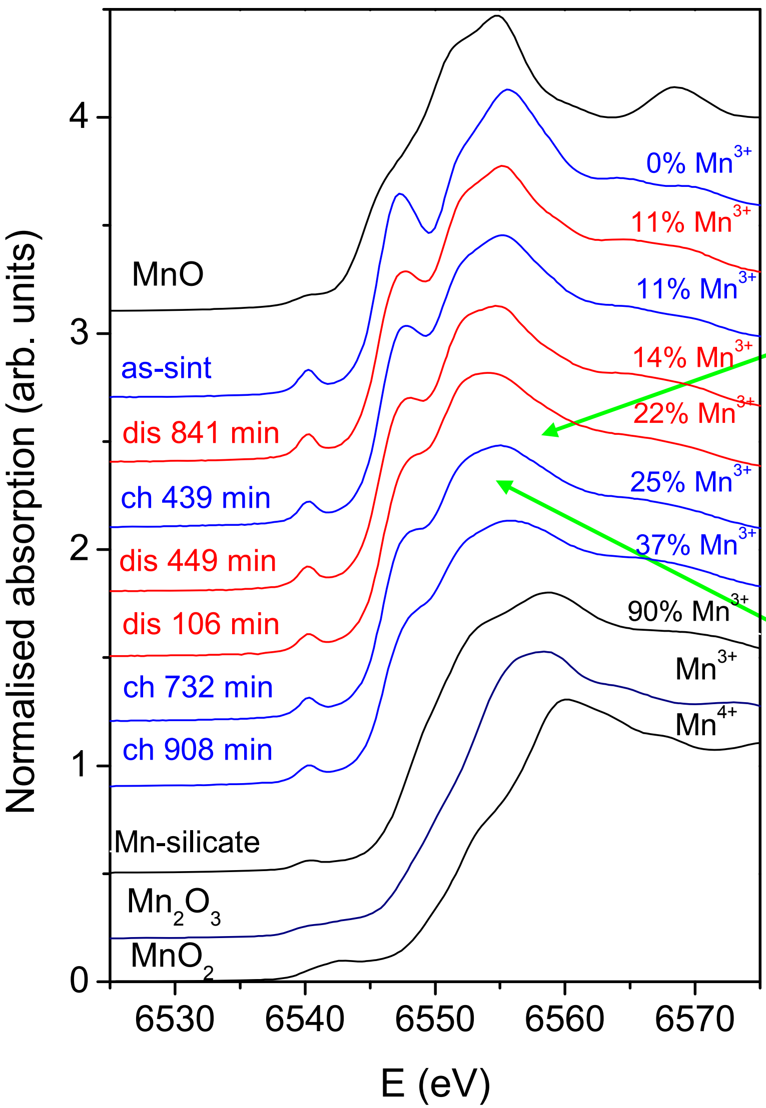

Linear combination fit with XANES spectra of "as-sint." and "ch. 908 min"

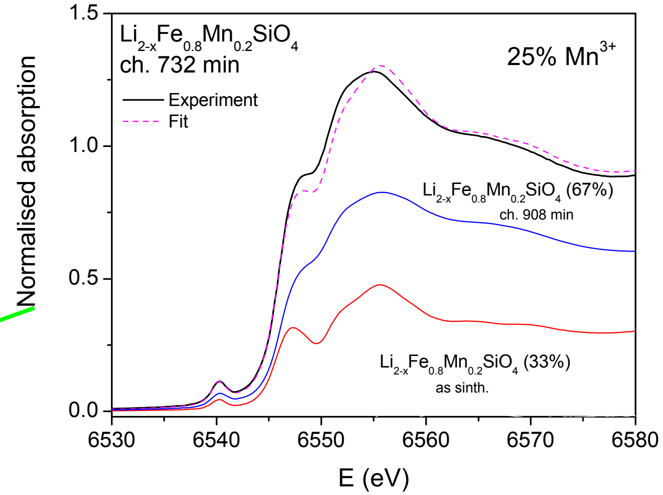

Linear combination fit with XANES spectra of "ch. 537 min " and "ch. 908 min"

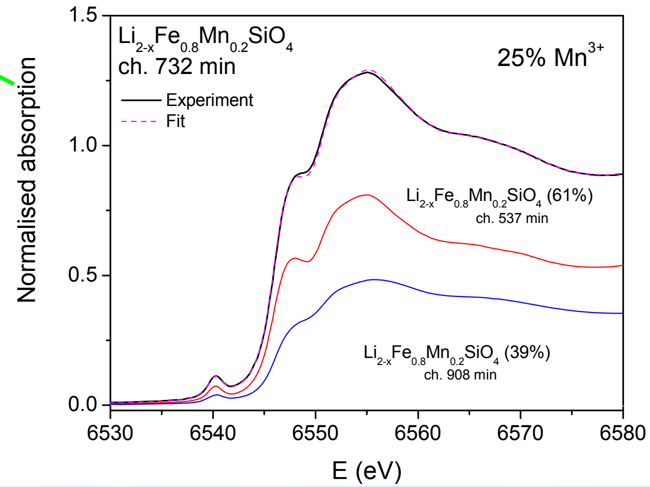

Relative amount of Fe^{3+} and Mn^{3+} in $Li_{2-x}(Fe_{0.8}Mn_{0.2})SiO_4$

during the the proces of battery charging and discharging

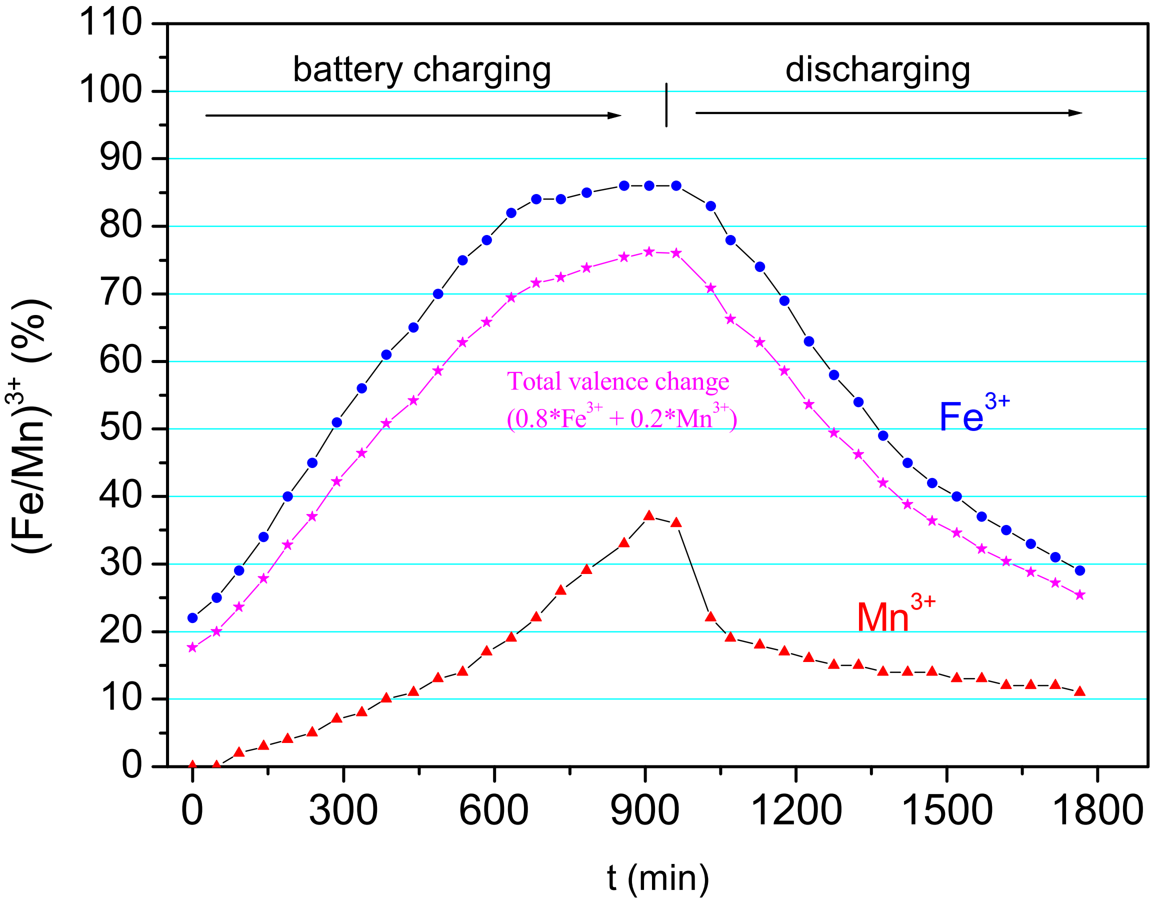

R. Dominko, C. Sirisopanaporn, C. Masquelier, D. Hanzel, I. Arcon, M. Gabersceka, Journal of The Electrochemical Society, 157 12 A1309-A1316 (2010)

Operando EXAFS analysis: monitoring local structure around Mn and Fe cations in $Li_2(Fe_{0.8}Mn_{0.2})SiO_4$ during battery operation

Fe/Mn neigh.	Coord. No.	Distance R(Å)
O	2	1.99
O	1	2.03
O	1	2.11
Li	1	2.79
O	1	2.92
Li	1	3.04
Si	1	3.05
Li	4	3.10
Si	2	3.13
Li	1	3.16
Si	1	3.18
…	…	…

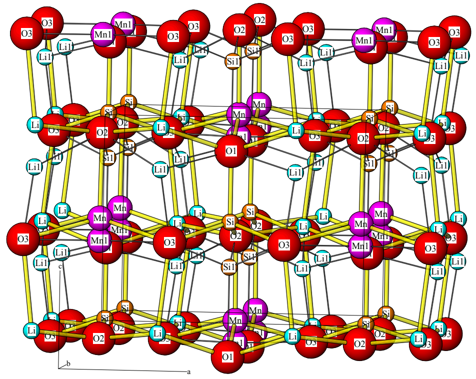

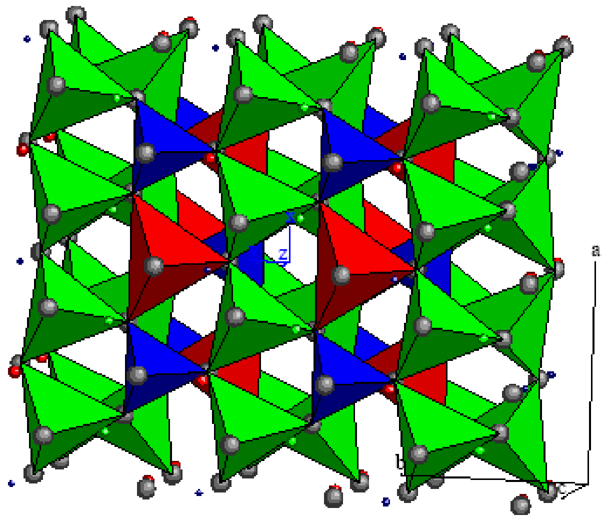

Initial structureobtained by powder XRD: monoclinic $\mathbf{Li_2(Fe_{0.8}Mn_{0.2})SiO_4}$ crystal structure with P121/n1 space group. a = 8.245 Å, b = 5.018 Å and c = 8.246 Å.

The structure is composed of MnO_4, FeO_4, SiO_4 and LiO_4 tetrahedra. R. Dominko, M. Bele, M. Gaberšček, A. Meden, M. Remškar, and J. Jamnik, *Electrochem. Commun.* **8**, 217 (2006).

Operando Fe EXAFS spectra of $Li_{2-x}Fe_{0.8}Mn_{0.2}SiO_4$

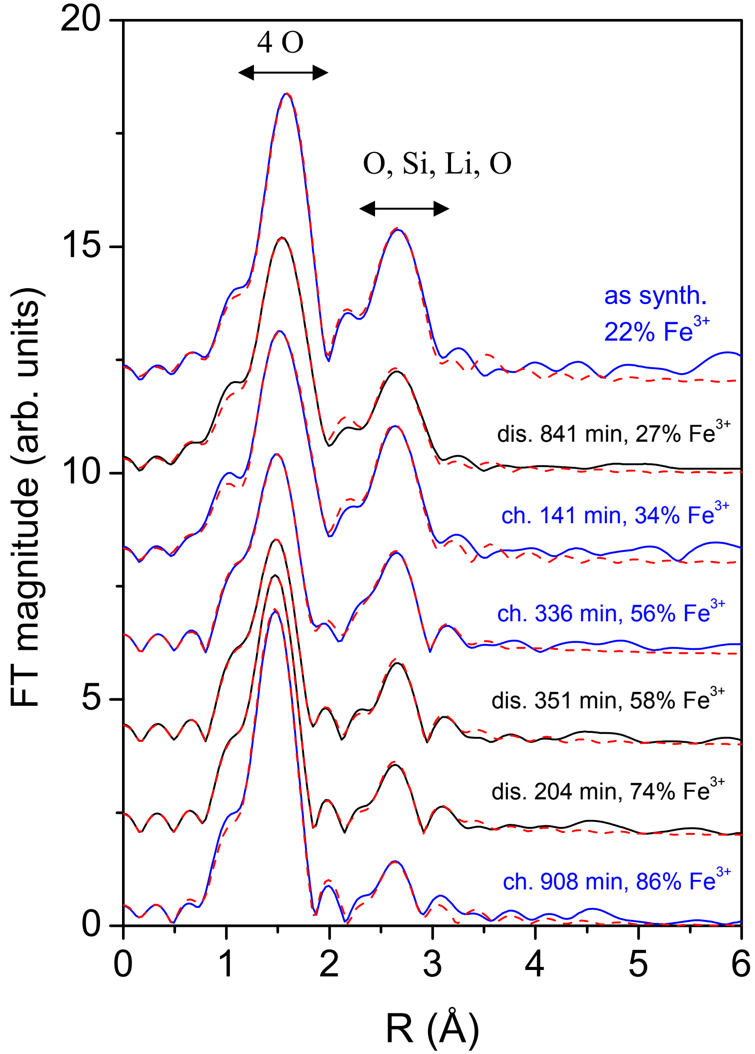

Changes of Fe local structure during charge/discharge process:

- modifications of FeO_4 tetrahedra
- increase of disorder in the second coordination shell

as synthesized
22% Fe^{3+}

1 **O** at 1.94 Å
3 **O** at 2.03 Å
$\sigma^2_{Fe-Si} = 0.009$ Å^2

reduced
27 % Fe^{3+}

4 O at 1.99 Å
$\sigma^2_{Fe-Si} = 0.008$ Å^2

Oxidized
86% Fe^{3+}

4 **O** at 1.88 Å
$\sigma^2_{Fe-Si} = 0.022$ Å^2

Experiment – (solid line); EXAFS model – (red dashed line)

R. Dominko, C. Sirisopanaporn, C. Masquelier, D. Hanzel, I. Arcon, M. Gabersceka, Journal of The Electrochemical Society, 157 12 A1309-A1316 (2010)

In situ Mn EXAFS spectra of $Li_{2-x}Fe_{0.8}Mn_{0.2}SiO_4$

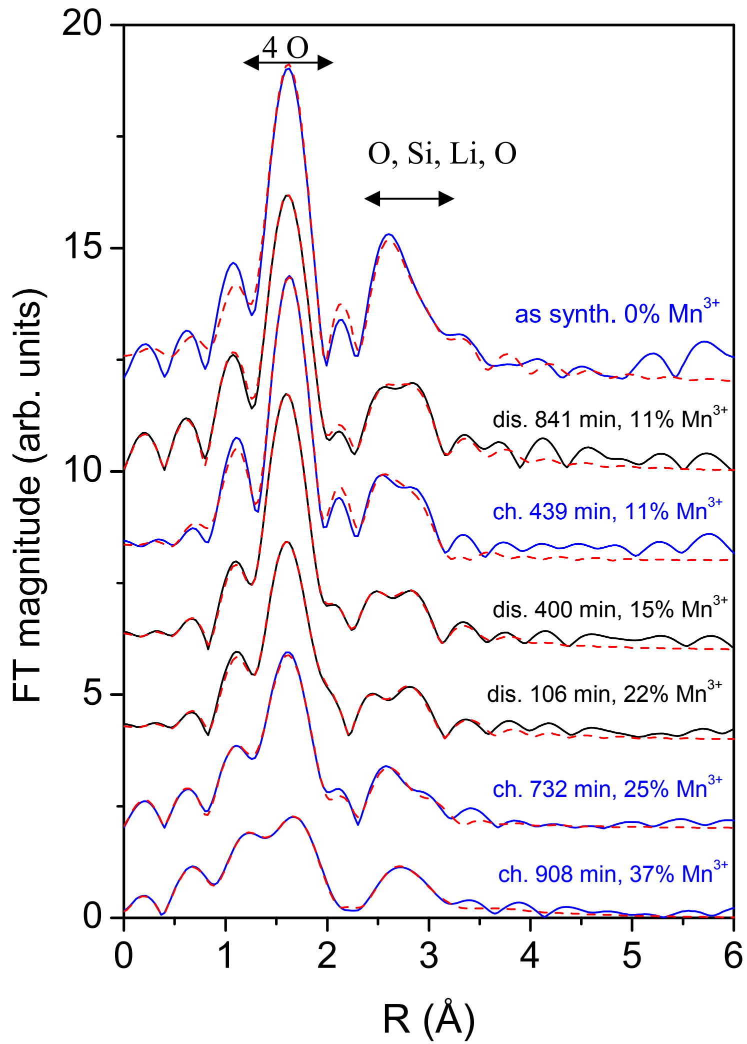

Experiment – (solid line); EXAFS model – (red dashed line)

Changes of Mn local structure during charge/discharge process:

- modifications of MnO_4 tetrahedra
- increase of disorder in the second coordination shell (Si)

as synthesized
0% Mn^{3+}

3 **O** at 2.04 Å
1 **O** at 2.21 Å
$\sigma^2_{Mn-Si} = 0.007$ Å^2

reduced
11 % Mn^{3+}

3 **O** at 2.04 Å
1 **O** at 2.17 Å
$\sigma^2_{Mn-Si} = 0.008$ Å^2

Oxidized
37% Mn^{3+}

1 **O** at 1.85 Å
3 **O** at 2.05 Å
$\sigma^2_{Mn-Si} = 0.016$ Å^2

XAS
Iztok Arčon

R. Dominko, C. Sirisopanaporn, C. Masquelier, D. Hanzel, I. Arcon, M. Gabersceka, Journal of The Electrochemical Society, 157 12 A1309-A1316 (2010)

Lithium sulphur batteries

are most promising solution for automotive applications

Charge / discharge
polysulphide shuttle mechanism

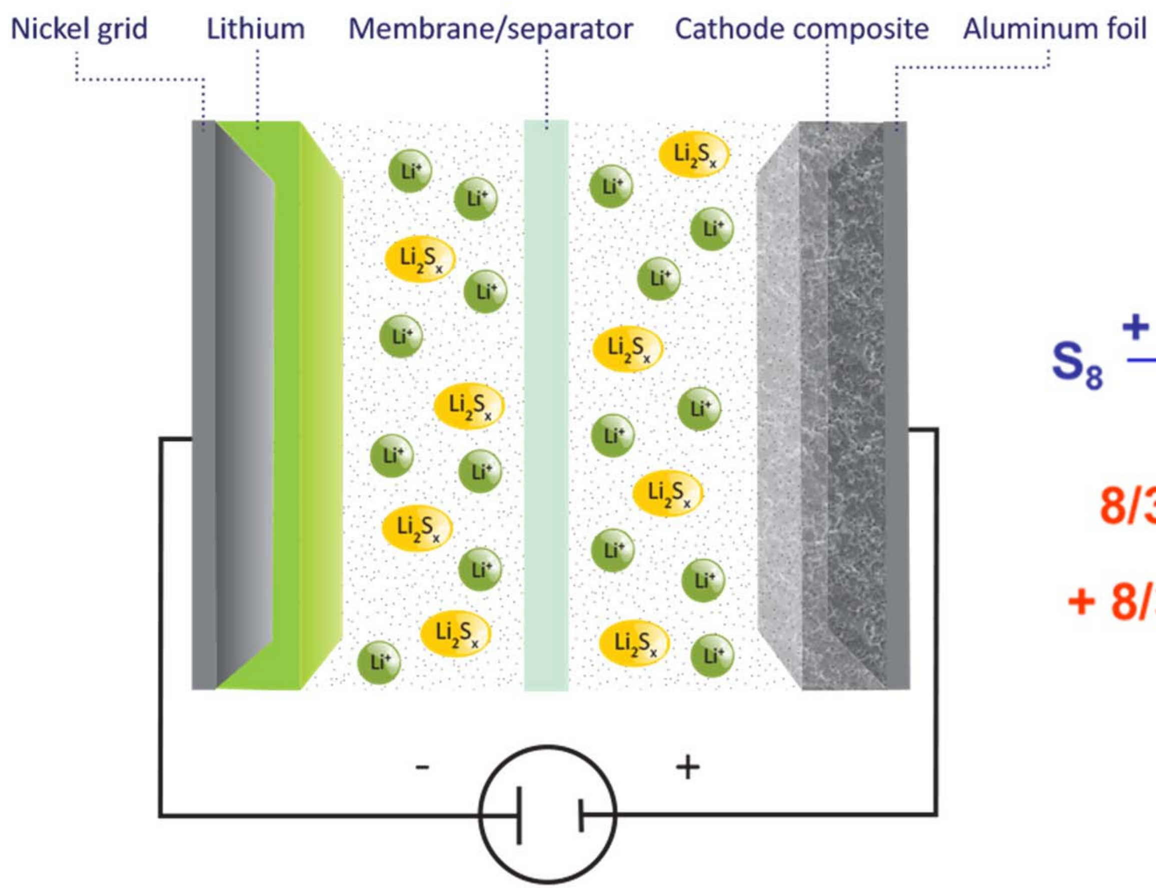

Cathode (sulphur)

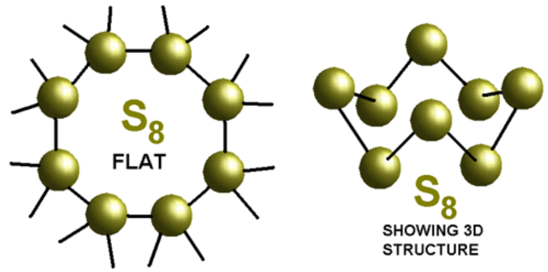

$$S_8 \xrightarrow{+2Li} Li_2S_8 \xrightarrow{+2/3Li} 4/3Li_2S_6$$

$$4/3Li_2S_6 \xrightarrow{+4/3Li} 2Li_2S_4 \xrightarrow{+4/3Li} 8/3Li_2S_3$$

$$8/3Li_2S_3 \xrightarrow{+8/3Li} 4Li_2S_2 \xrightarrow{+2Li} 8Li_2S$$

Aim of operando XAS study of Li-S battery

OperandoSulphur K-edge XANES and EXAFS analysis of Li-S batteries as a tool for:

- characterization of the redox chemistry during charging and discharging of the battery.
- information on changes in the **molecular structure of sulphur** and **sulphur oxidation state** in the cathode material.
- **monitoring polysulfide formation** to understand the interactions of sulfur and polysulfides with a host matrix and electrolyte.

This information is esential for the development of long cycle life of lithium sulfur (Li-S) batteries.

Experimental: setup

Fluorescence detection mode ($\mu(E) \propto I_F/I_0$) at Sulphur K-edge (2472 eV)
XAFS beamline at Elettra

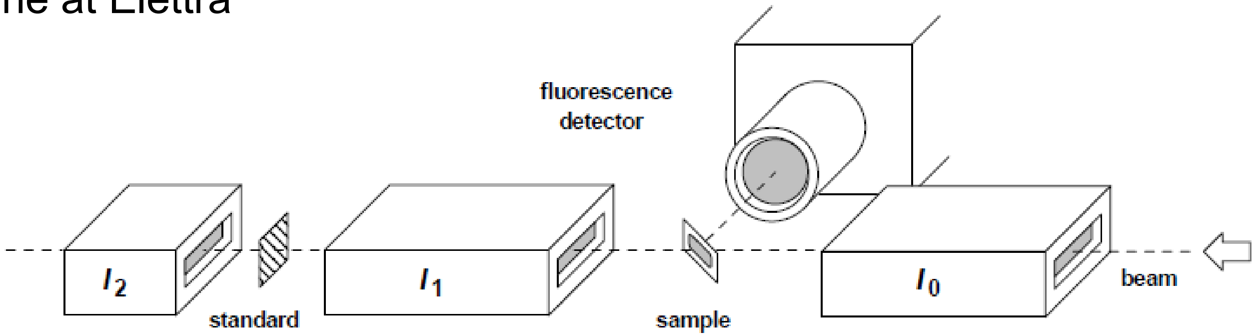

Samples in vacuum
or helium atmosphere

Modified 4-electrode Swagelok cell
for in operando XAS measurenets
with 13 micron Be window

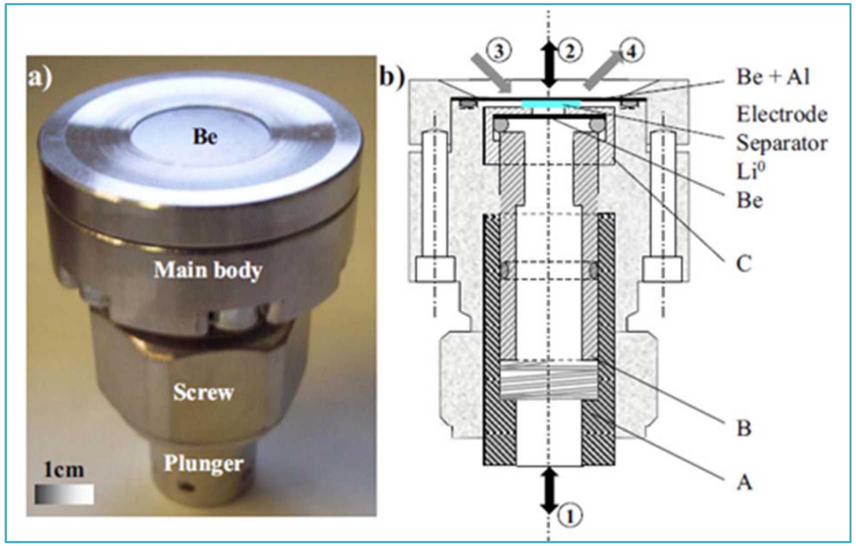

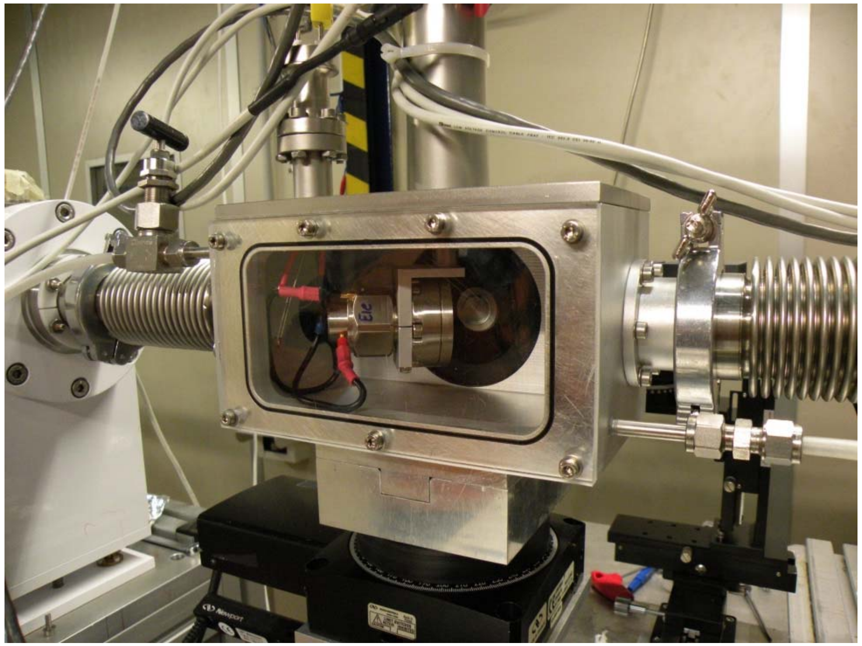

In opearndo XAS measurement on Li-S battery

Battery cathode with 20% of S in carbon composite cathode
with 3.5% zeolite, electrolyte without sulphur (LiTDI)

In operando S K-edge XANES on battery

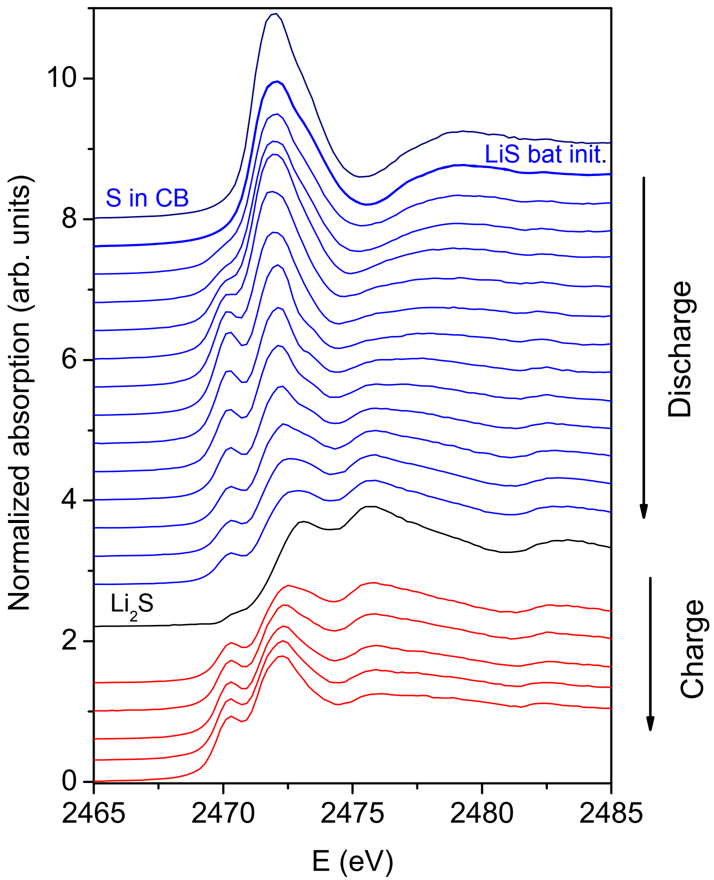

S K-edge EXAFS of refrence sulphur compounds

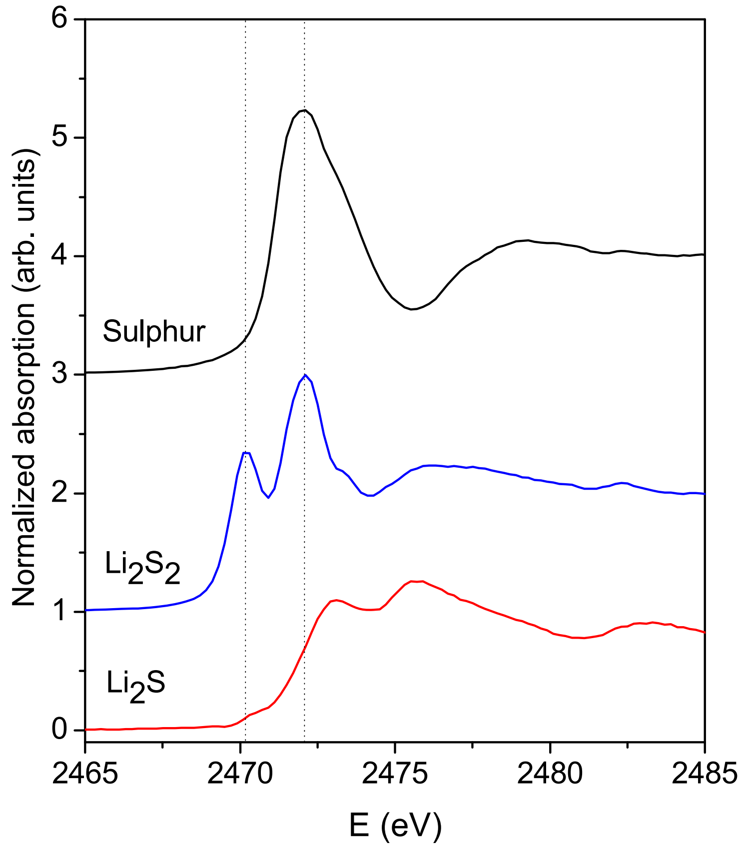

Discharging rate C/40, Charging rate C/15

In opearndo S K-edge XANES analysis

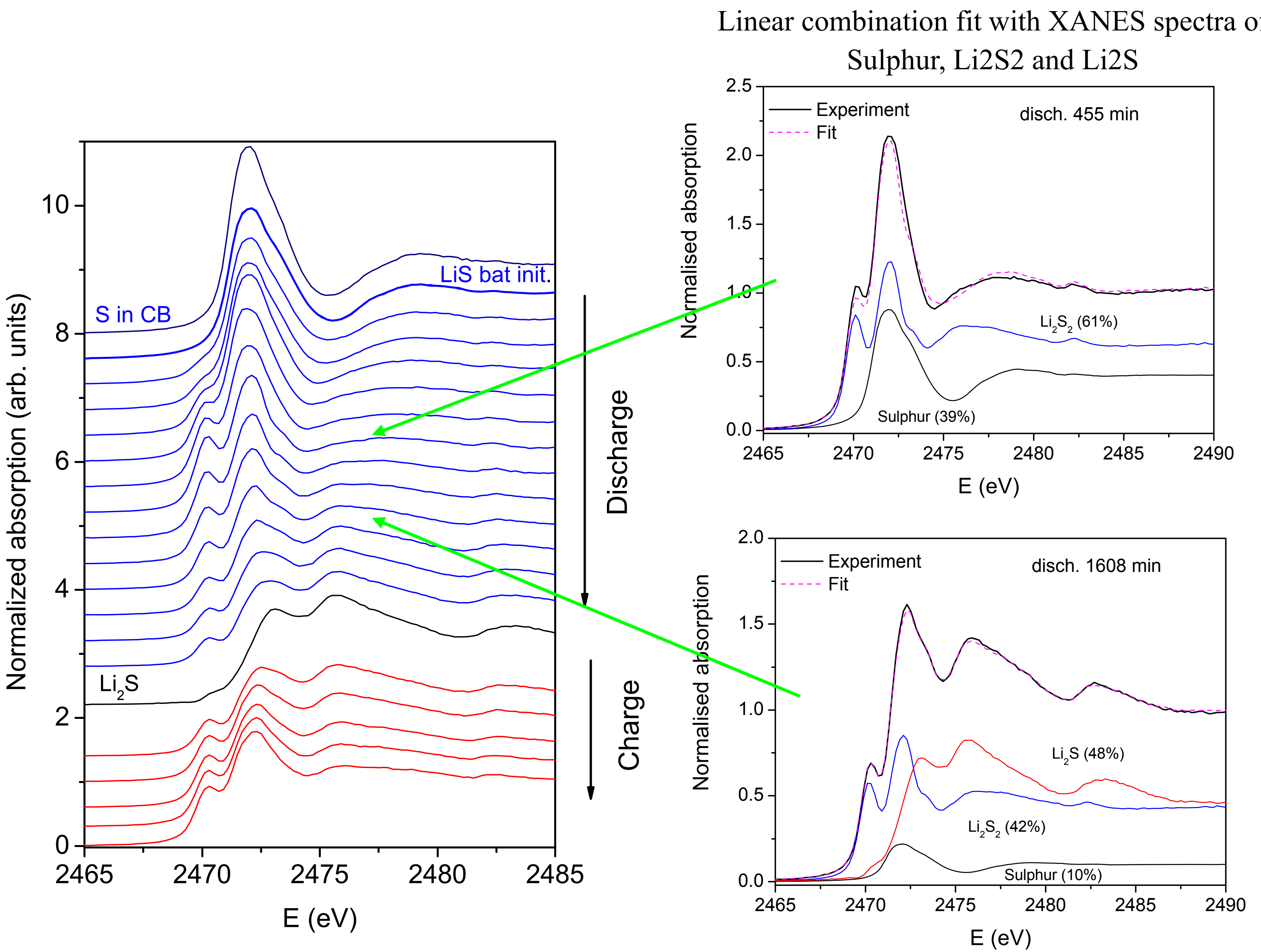

In opearndo S K-edge XANES analysis

Linear combination fit with XANES spectra of Sulphur, Li2S2 and Li2S

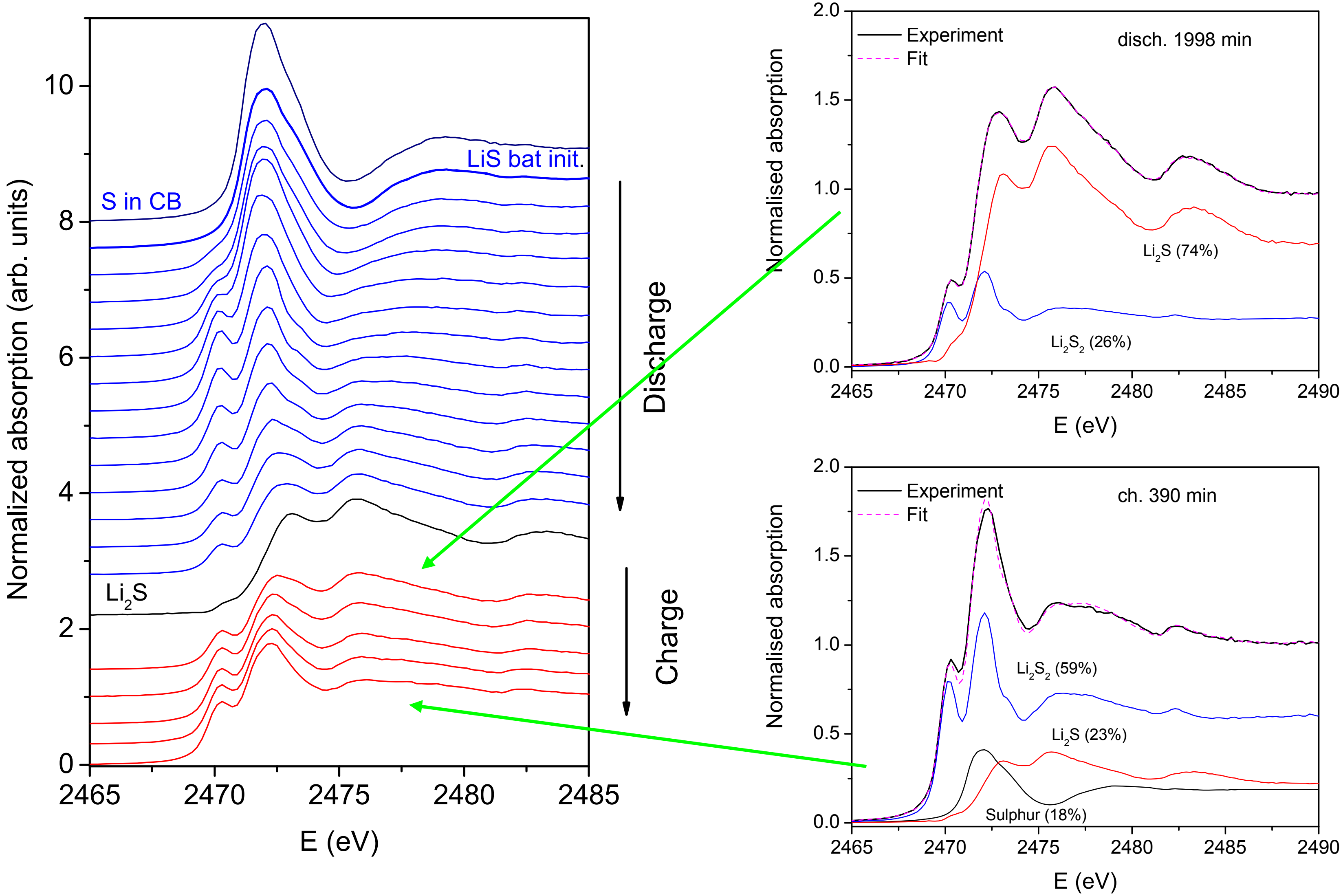

In opearndo S K-edge XANES analysis

Relative amount of three different sulphur compounds sulphur, Li2S2 and Li2S in the cathode during 1st cycle ob battery opeartion

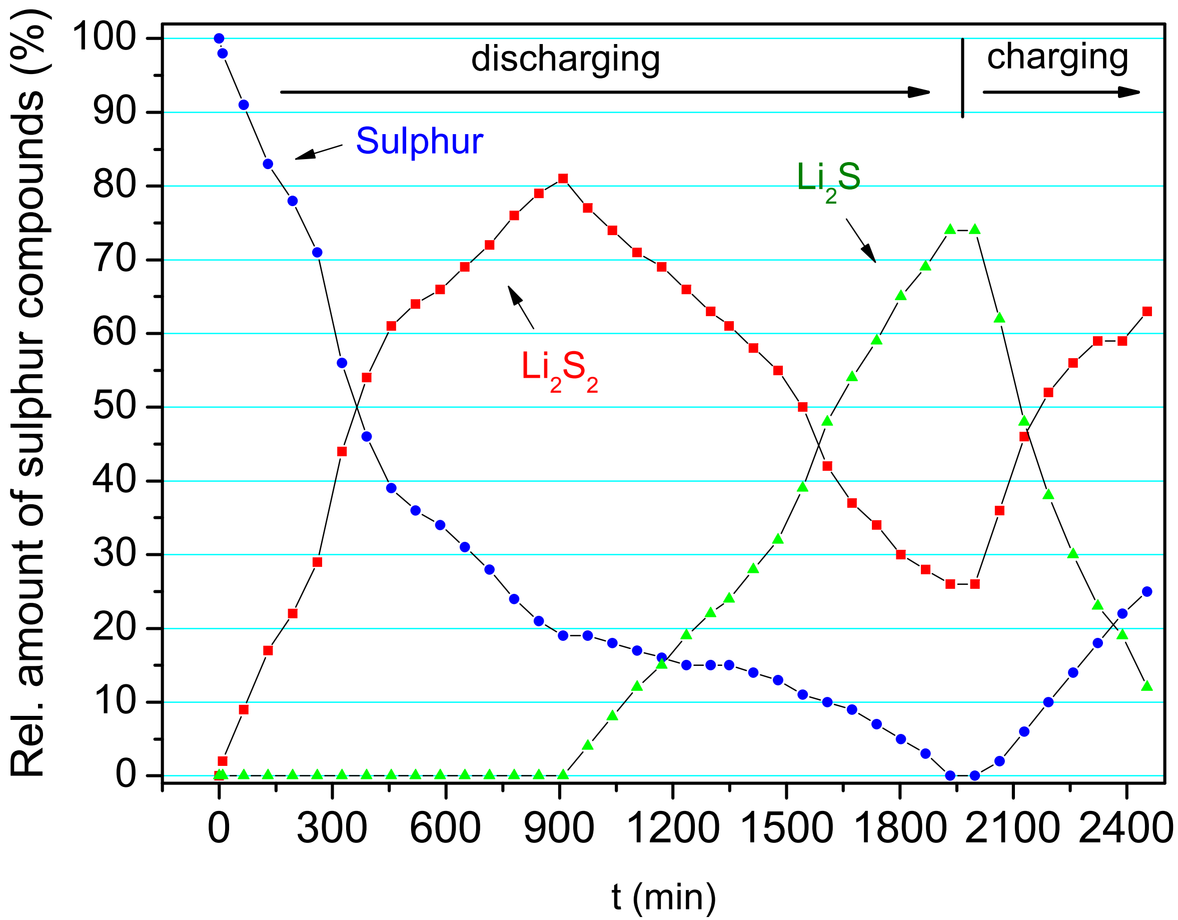

R. Dominko, M. Ubrani, M. Patel, V. Lapornik, A. Vižintin, M.Koželj, N. Novak Tušar, I, Arčon, L. Stievano, G. Aquilanti, Analytical detection of polysulfides in the presence of adsorption additives by operando X-ray absorption spectroscopy *The journal of physical chemistry. C, Nanomaterials and interfaces*, ISSN 1932-7447, vol. 119, iss. 33, (2015) 19001-19010, doi:10.1021/acs.jpcc.5b05609.

In opearndo S K-edge EXAFS analysis

Battery cathode with 20% of S in carbon composite cathode
with 3.5% zeolite, electrolyte without sulphur (LiTDI)

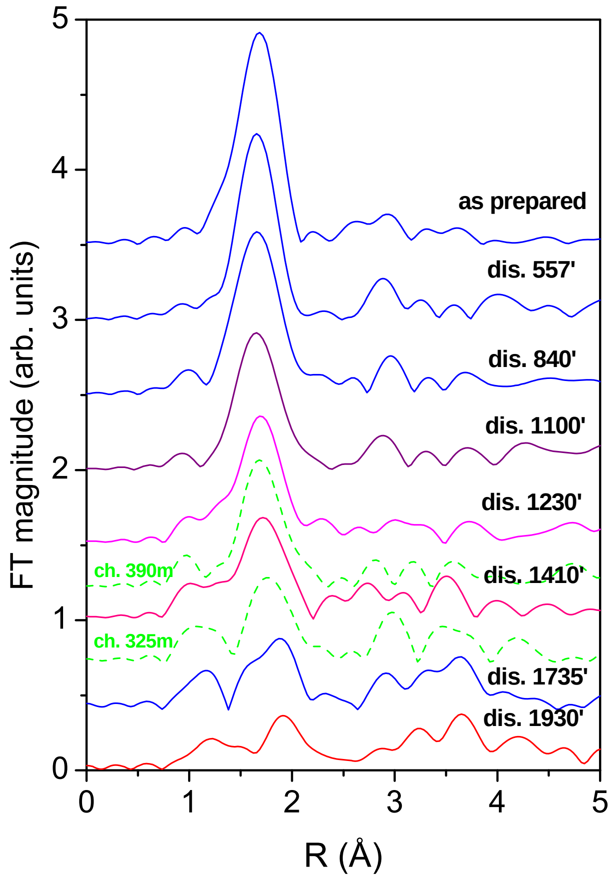

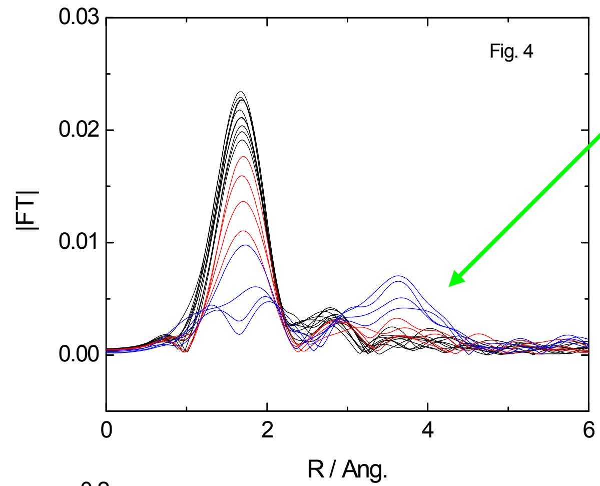

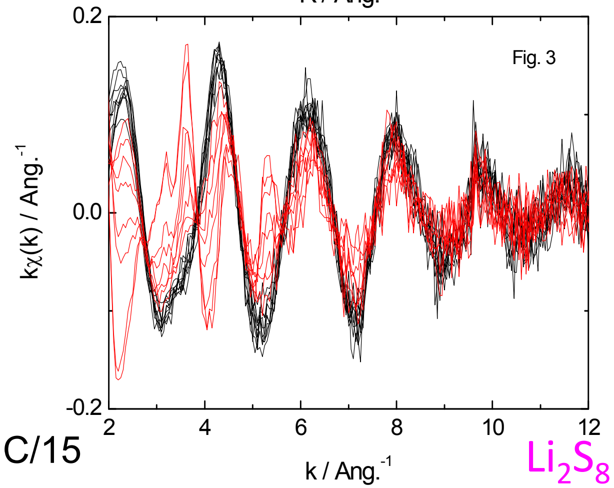

The formation of **Li2S** in the antifluorite structure is visible by the appearnce of a clear second neighbour peak in FT EXAFS spectra. (blue curves)

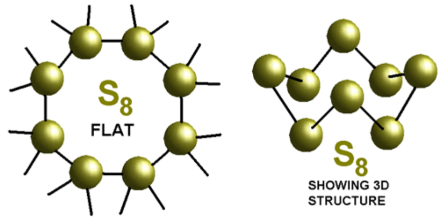

Discharging rate C/40, Charging rate C/15

Li_2S_8 :   Li—S-S-S-S-S-S-S-S—Li

Li_2S_3 :   Li—S-S-S—Li

Li_2S_2 :   Li—S-S—Li

Li_2S :   Li—S—Li

R. Dominko, M. Ubrani, M. Patel, V. Lapornik, A. Vižintin, M.Koželj, N. Novak Tušar, I, Arčon, L. Stievano, G. Aquilanti,
The journal of physical chemistry. C, Nanomaterials and interfaces, ISSN 1932-7447, vol. 119, iss. 33, (2015) 19001-19010, doi:10.1021/acs.jpcc.5b05609.

Micro-XRF mapping, micro-XANES and EXAFS

tools for characterization of metal cations in plants on subcellular level

Metal pollution

Metal cations (Cd, Zn, Pb, As, Hg, ..) are extremely toxic even at low concentrations. They are easily taken up from polluted soil by plants and translocated to the food chains.

Biofortification

Increase concentrations of essential elements (Fe) in the edible plant parts.

WHO: Fe deficiency is the most common nutritional disorder in the world, affecting nearly 30% of the world's population

Goal: Understand mechanisms of uptake, transport, accumulation and complexation of metal cations in metal hyper-accumulating and non-accumulating plants.

Benefit: Enhance phytoextraction efficiency with hyper-accumulating plants to improve phytoremediaition techniques for polluted soils.

Benefit: Enhance biofortification technologies and improve crop yields.

Metal pollution

Soil - Žerjav

Pb: ~ 50,000 mg kg^{-1}

Zn: ~ 4000 mg kg^{-1}

Cd: ~ 150 mg kg^{-1}

Critical levels

Pb: 530 mg kg^{-1}

Zn: 720 mg kg^{-1}

Cd: 12 mg kg^{-1}

Soil – Mežica- gardens

Pb: ~ 2,000 mg kg^{-1}

Zn: ~2,700 mg kg^{-1}

Cd: 10-25 mg kg^{-1}

remediation

Regvar et al. 2006. *Environmental pollution 144,976-984*

Metal hyperaccumulating plants

Thlaspi praecox

5960 mg kg^{-1} Cd

14590 mg kg^{-1} Zn in shoots

Physiological mechanisms of coping with excess metals in tissues?

Vogel-Mikuš et al. 2005. *Environmental pollution 133, 233-242*

Vogel-Mikuš et al. 2006. *Environmental pollution 139, 362-371*

Free Cd2+ metal cations are toxic already at low concentrations.

Questions

- **What are tolerance mechanisms in hyperaccumulating plants?**
- **What are complexation mechanisms at biochemical level?**

- **Where are toxic cations stored in plant cells?**
- **How is Cd bonded in different plant tissues?**

Element localization studies on subcellular level µ-XRF and Cd L3-edge µ-XANES; ID 21, ESRF Grenoble

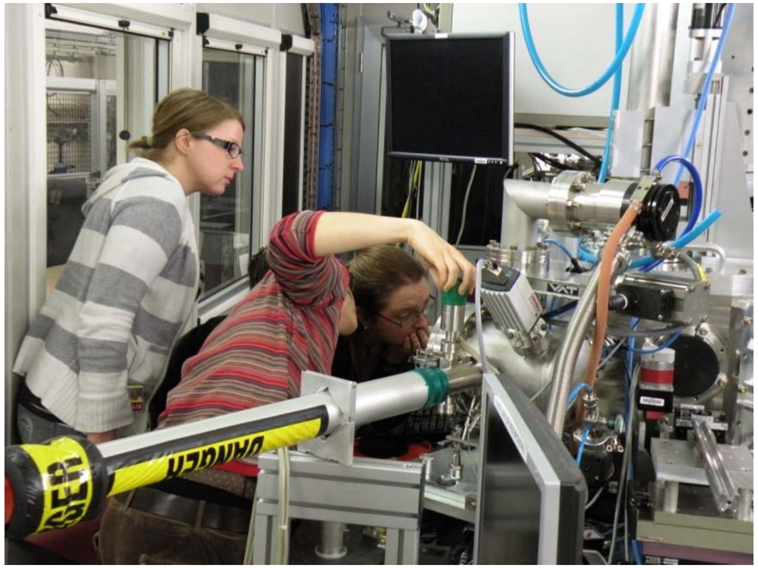

Scanning transmission X-ray microscope (1-9 keV)
Monchromatic beam focused to
0.3 x 0.7 µm^2
using zoneplate micro focusing.

- Localization of elements
- Micro-XANES analysis

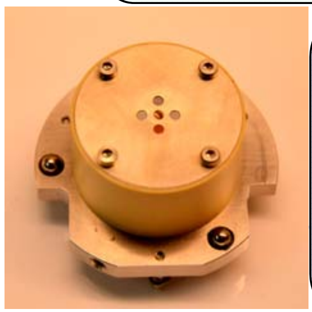

Cryo-fixed freeze-dryed samples, mounted between two Ultralene foils

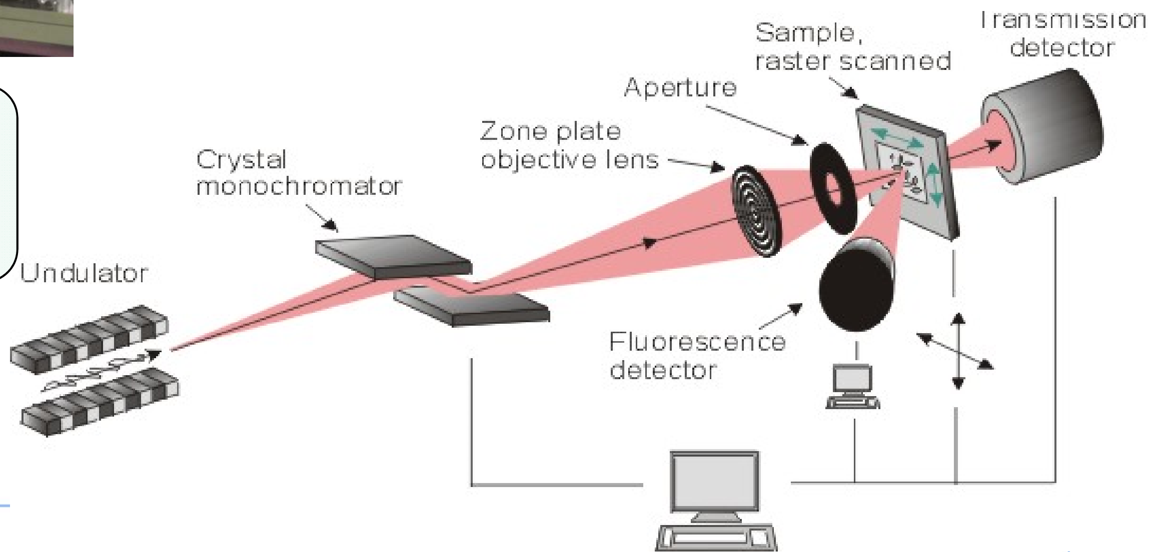

Micro-XRF mapping – ESRF, ID21

Excitation energy 3.55 keV; mapping on Cd-L3 line with 1μm^2 beam

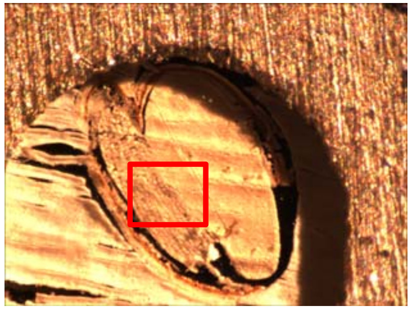

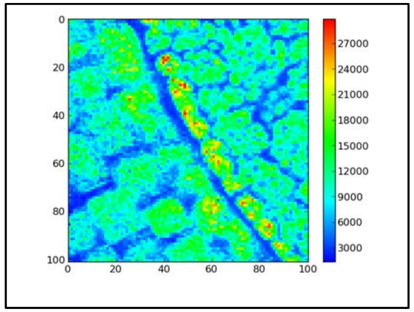

QUANTITATIVE ANALYSIS, based on fundamental parameters; QA-MICRO-XRF software, Peter Kump ©, IJS

- Intensity of emitted X-ray lines
- Sample density determined from scattering; /matrix composition = cellulose

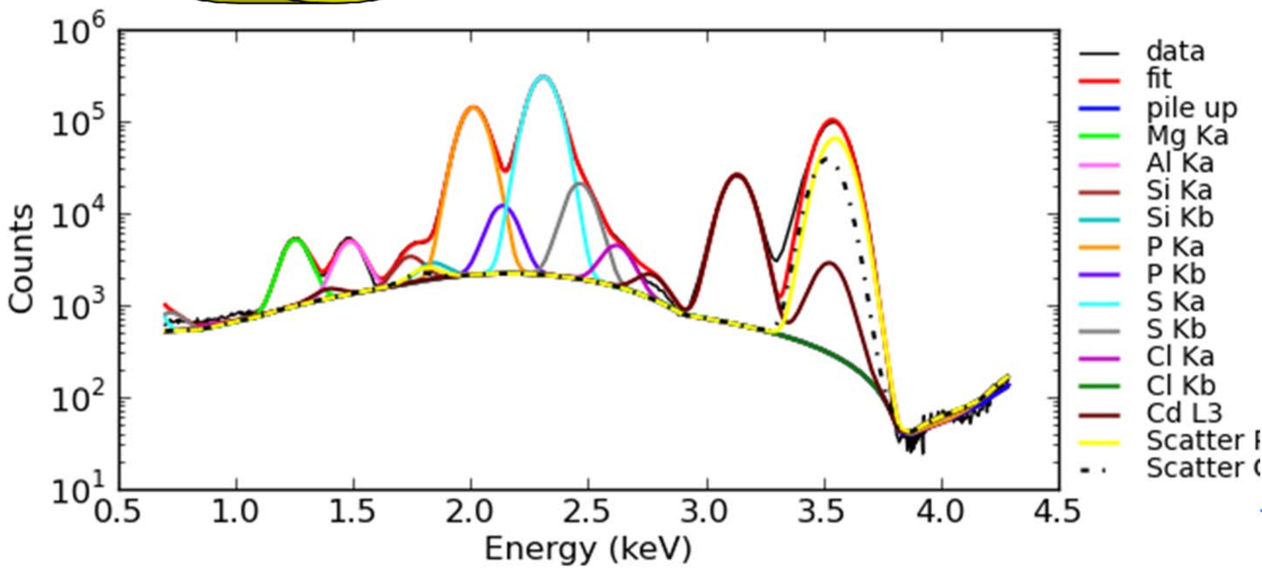

Cd L3-edge XANES

Linear combination fit is of Cd L3-edge XANES can provide more information on Cd complexation.

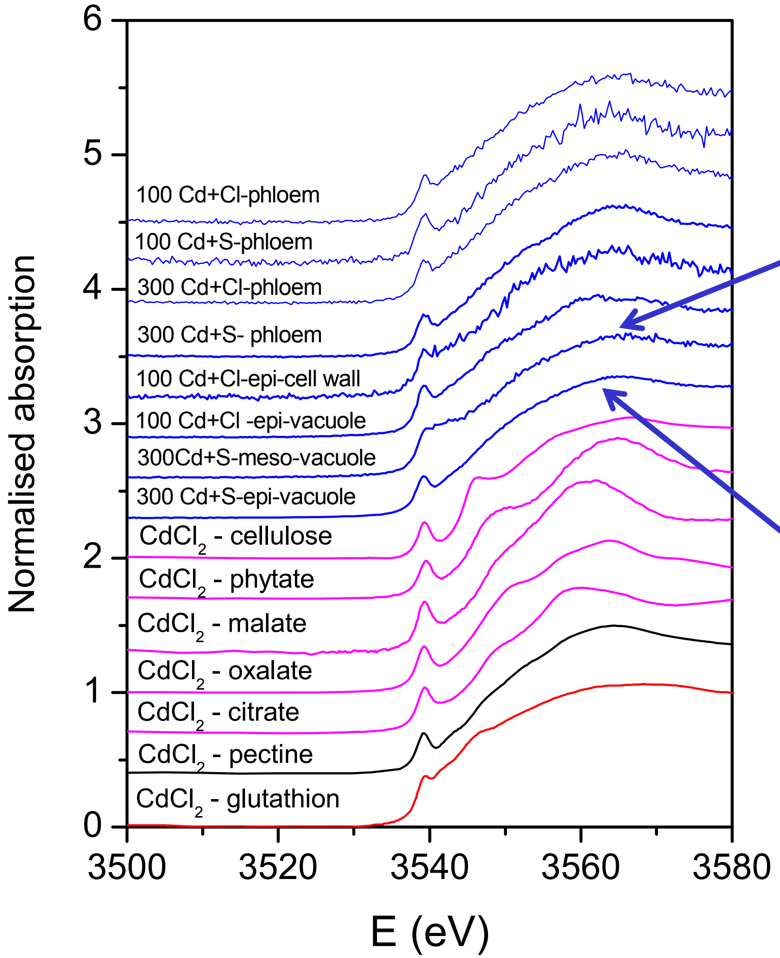

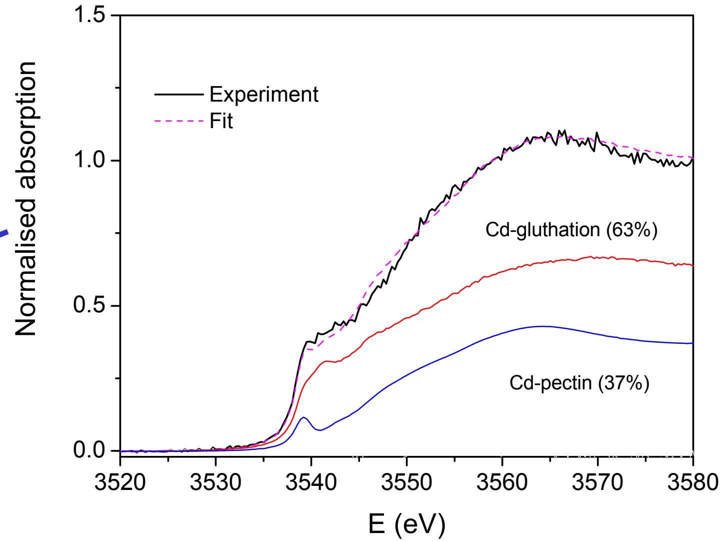

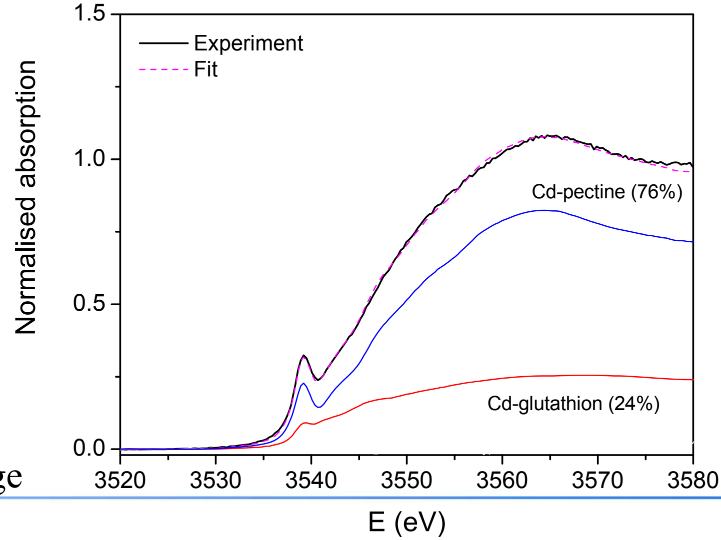

Cd L3 edge natural width 2.50 eV, sharp features at the edge are clearly resolved.

Micro XRF - Localization and ligand environment of Cd in leaves of hydroponically grown Cd hyperaccumulator *T. praecox plants*;
mapping above Cd-L3 edge at 3.55 keV;
ID21, ESRF, Grenoble

Epidermal cells

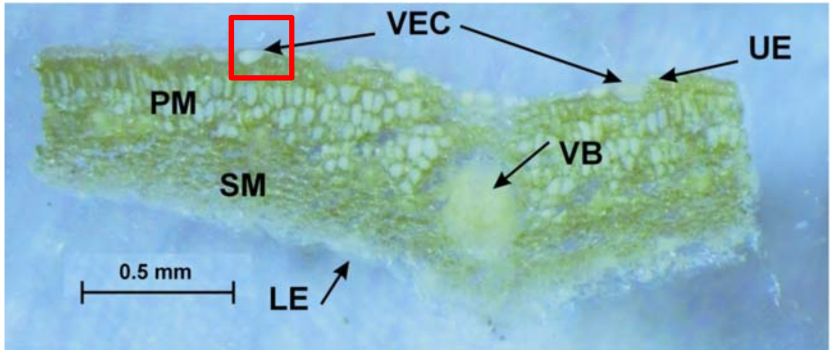

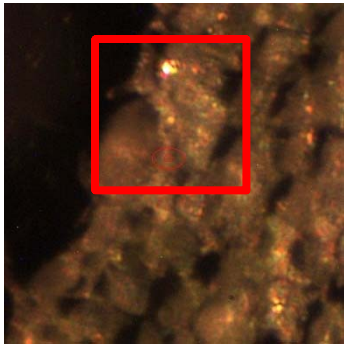

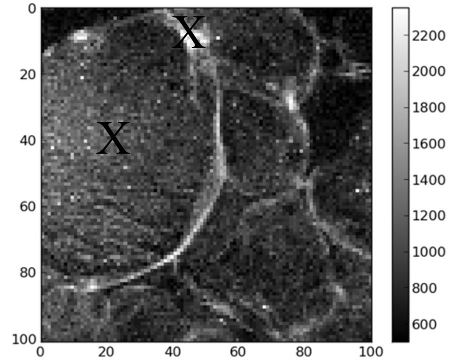

ρd

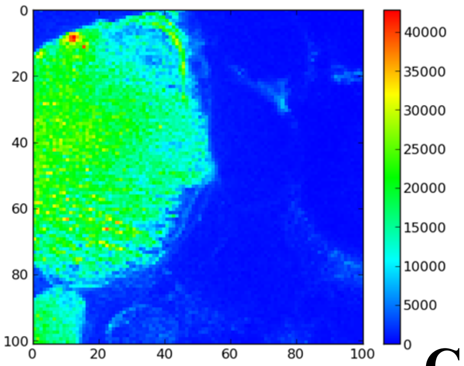

Cd

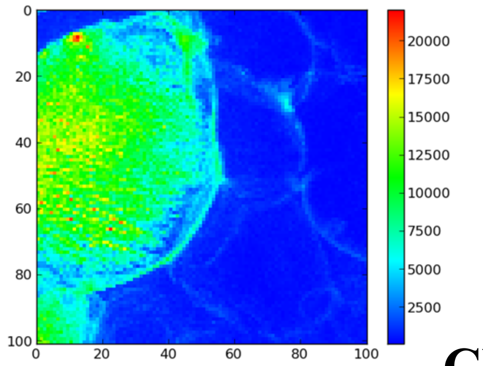

Cl

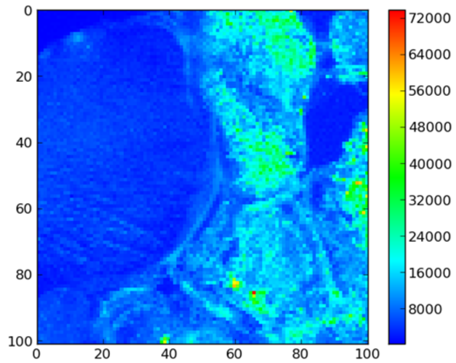

S

Vacuolar compartmentation **of Cd in epidermal cells**

Colocalization analysis and Cd-L3 micro-XANES in epidermal cells of *T. praecox plants*

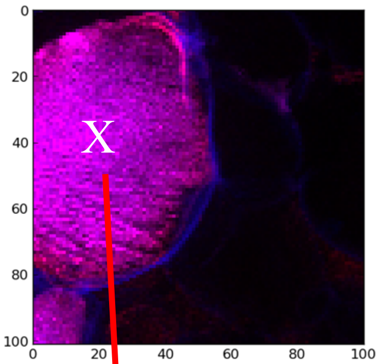

Cd (red) Cl (blue) – colocalised (magenta)

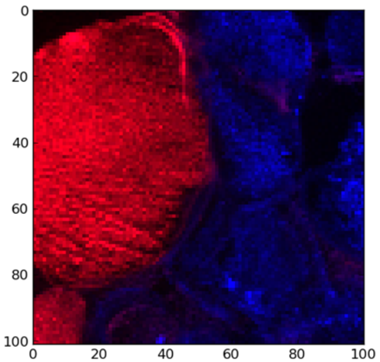

Cd (red)-S (blue)

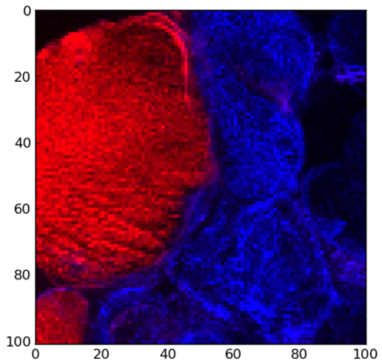

Cd (red)-P (blue)

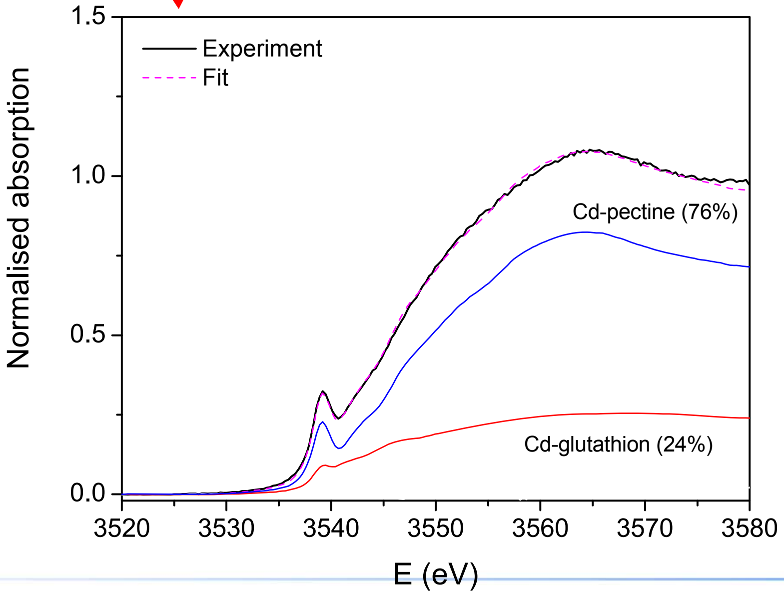

Cd – pectinate: Cd-O-OC and Cd-O-C coord.

Cd-GSH : Cd-S-C coord

Epidermis - vacuole	
Standard	Contribution (%)
Cd-pectinate	76 %
Cd-GSH	24 %

Localization and ligand environment of Cd in mesophyll cells
In leaves of hydroponically grown Cd hyperaccumulator *T. praecox plants*

micro XRF mapping above Cd-L3 edge at 3.55 keV; ID21, ESRF, Grenoble

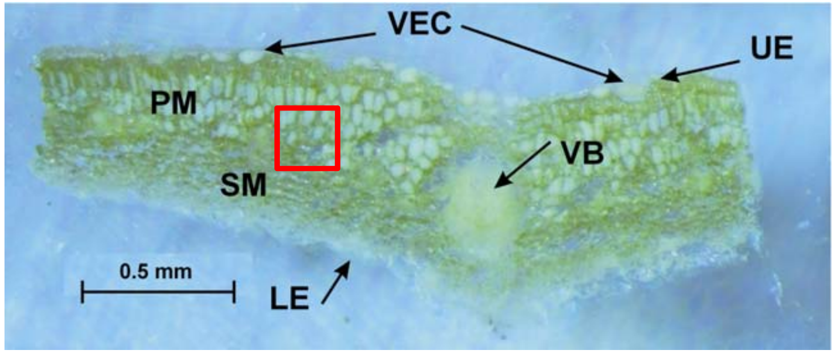

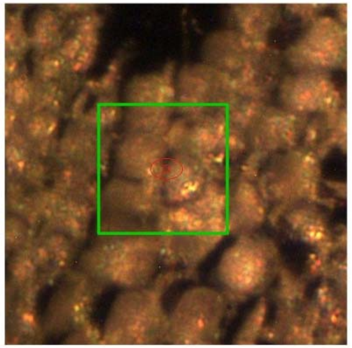

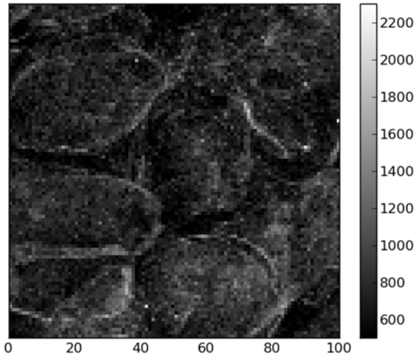

Mesophyll cells

ρd

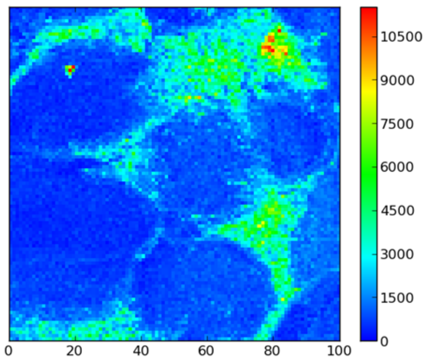

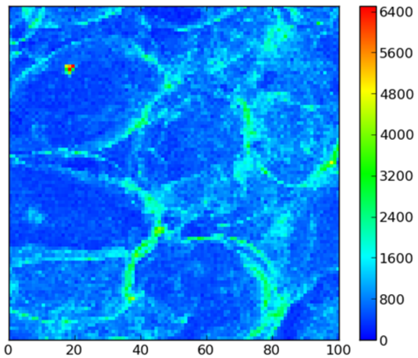

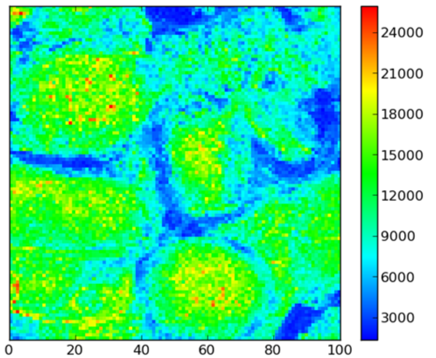

Cd

Cl

S

***Cell wall compartment of Cd in* mesophyll cells**

(QA-micro-XRF © P. Kump, IJS)

Colocalization analysis and Cd-L3 micro-XANES in Mesophyll cells of *T. praecox plants*

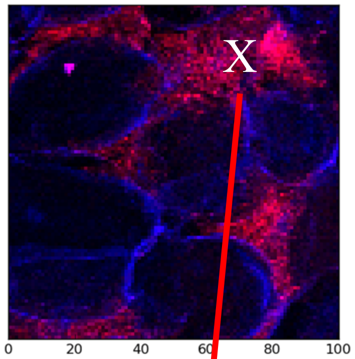

Cd (red) Cl (blue) colocalised (magenta)

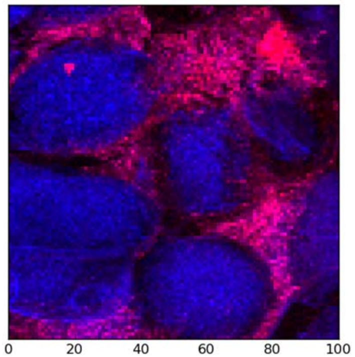

Cd (red)-S (blue)

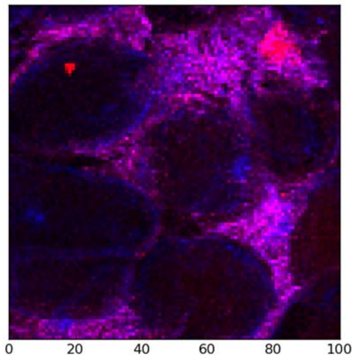

Cd (red)-P (blue)

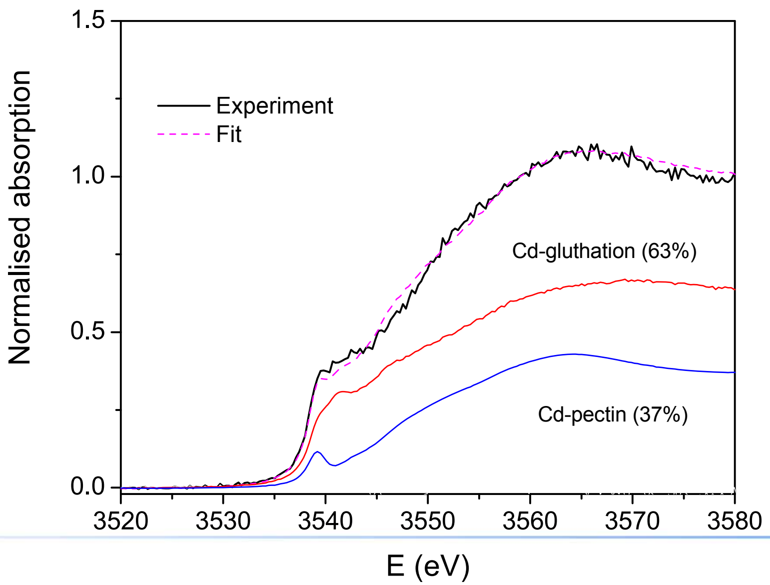

Cd – pectinate: Cd-O-OC and Cd-O-C coord.

Cd-GSH : Cd-S-C coord.

Mesophyll – cell wall	
Standard	Contribution (%)
Cd-pectinate	37%
Cd-GSH	63%

Results: Cd hyper-accumulating plants

- In leaves the main tolerance mechanisms to high Cd concentrations are ***vacuolar compartmentation (in epidermal cells)*** and ***binding to the cell wall components (in mesophyll cells)*** .
- Cd binds in tissues to ***oxygen and sulphur ligands***, but not to chlorine or phosphorus.

Š. Koren, I. Arčon, P. Kump, M. Nečemer, K. Vogel-Mikuš, Plant Soil 370, no. 1/2, (2013) 125-148
DOI 10.1007/s11104-013-1617-0,

3D micro-XRF mapping of elements

Confocal X-ray microscope fro 3D mapping.

Diameter of the beam in focusu is about 10-30 microns

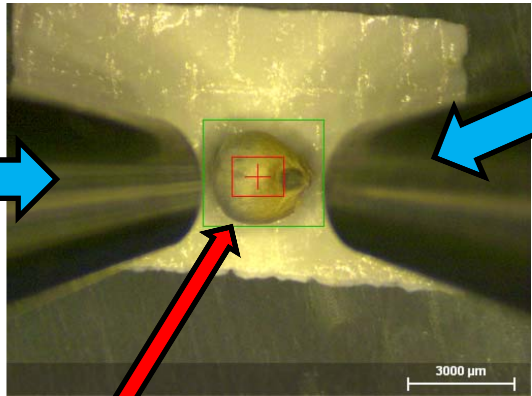

Polycapilary lense in front of the detector for X-ray fluorescence light.

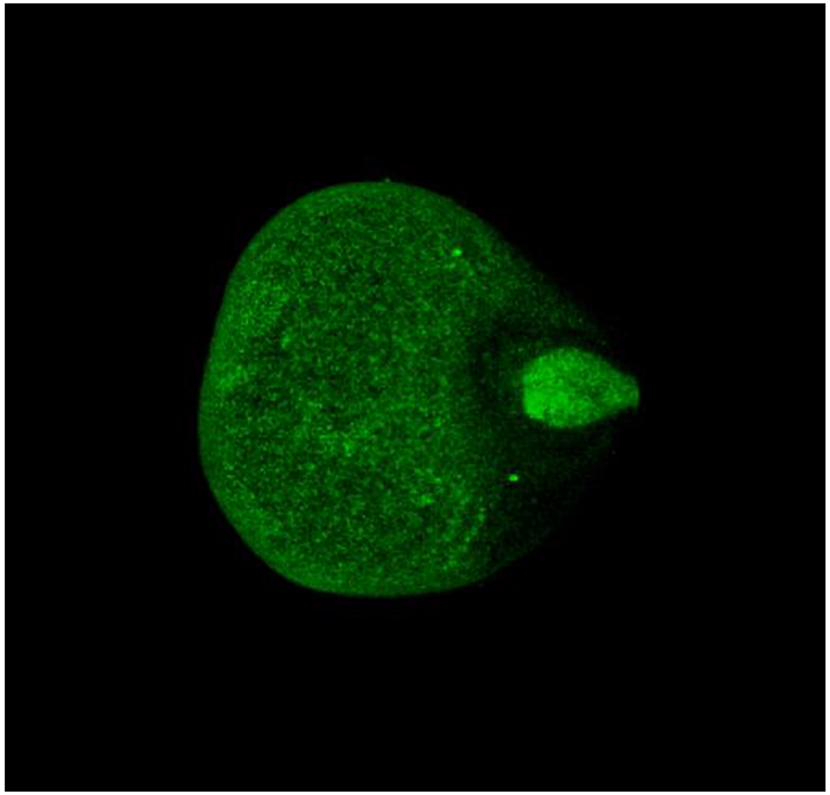

Grain of millet (visible light microscope)

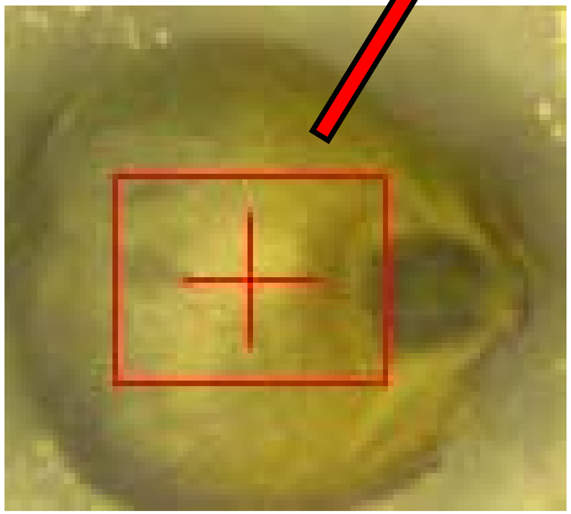

3D distribution of Fe in on the surface of millet. Measured at TU Berlin.

B. Kanngiesser, I. Mantouvalou

3D micro-XRF mapping of elements

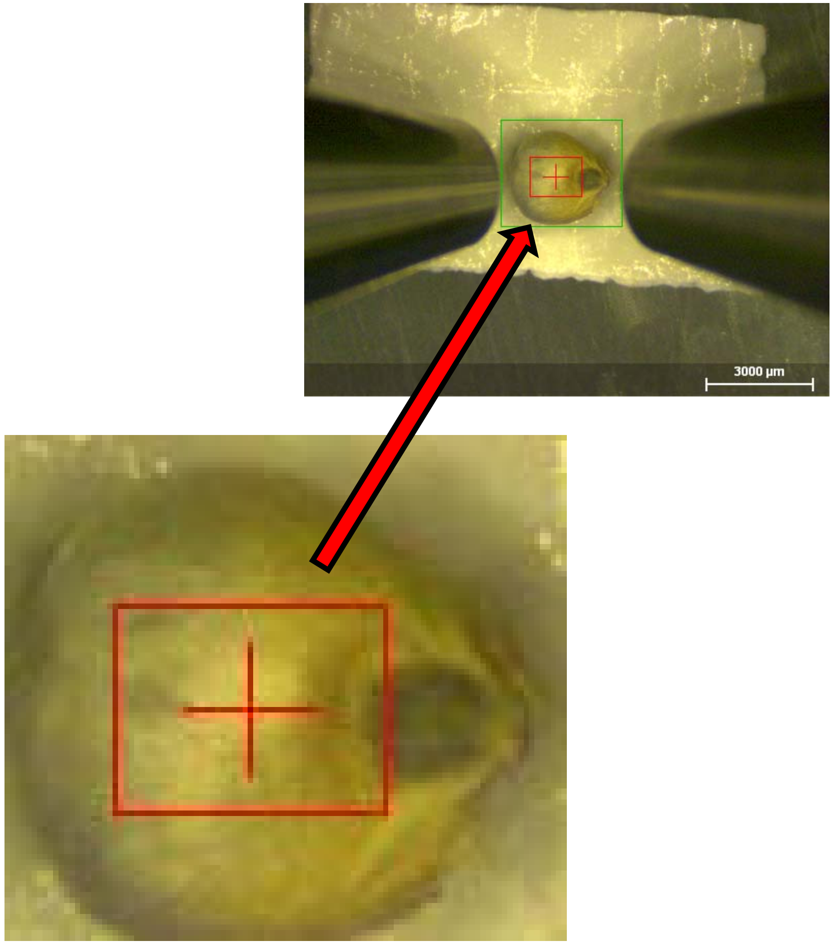

Grain of millet (visible light microscope)

3D distribution of K, Ca and Fe in millet.

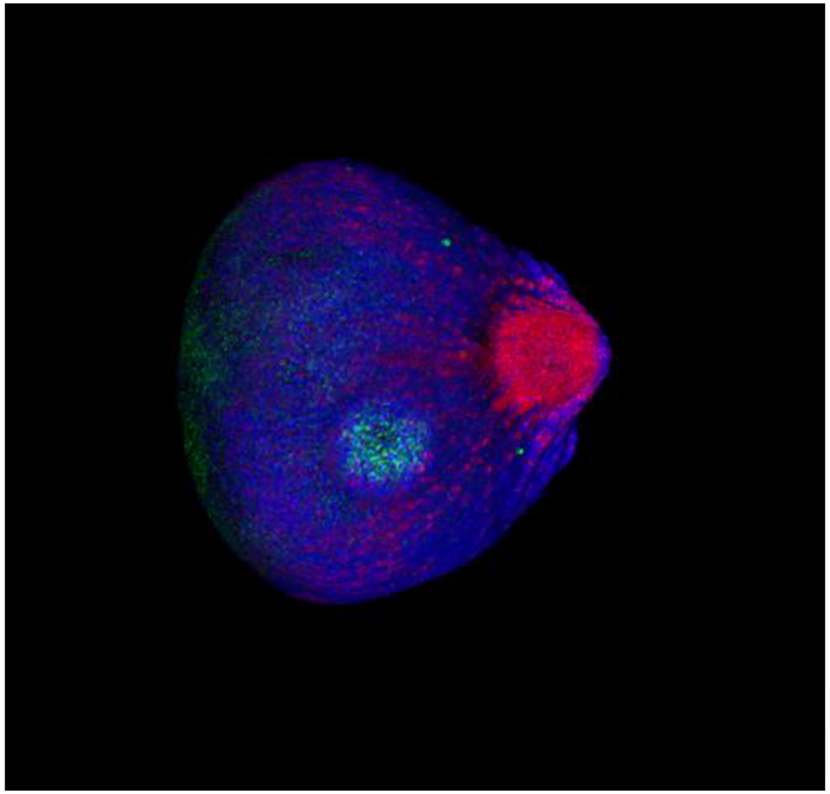

Measured at TU Berlin.

B. Kanngiesser, I. Mantouvalou

Acknowledgements

This work was supported by:

- Slovenian Research Agency
- EC project **EUROLIS** (314515) FP7-2012-GC-MATERIALS
- DESY and the European Community's FP7 Programme (FP7/2007–2013) under grant agreement CALIPSO No :312284 (EU Support of Access to Synchrotrons/FELs in Europe).
- HASYLAB, ESRF and ELETTRA, who provided access to their synchrotron radiation facilities
- IAEA framework of coordinated research projects RC 13858 "Unification of nuclear spectrometries: integrated techniques as a new tool for materials research"
- RC 16796 "Applications of synchrotron radiation for environmental sciences and materials research for development of environmentally friendly resources"

Coworkers:

✓ Katarina Vogel-Mikuš
✓ Peter Kump
✓ Edmund Welter (HASYLAB)
✓ Giuliana Aquilanti (ELETTRA)
✓ Luca Olivi (ELETTRA)
✓ Hiram Castillo-Michel (ESRF)
✓.Robert Dominko (Inst. Of Chemistry, Lj.)
✓ Manu Patel (Inst. Of Chemistry, Lj.)
✓ Lorenzo Stievano (Université Montpellier II)
✓B. Kanngiesser, (TU Berlin)
✓I. Mantouvalou (TU Berlin)

ID21 beamline, ESRF

XAFS beamline, ELETTRA